EXAMINATION OF CRYSTAL RIVER-3 PULLED STEAM GENERATOR TUBES
FINAL REPORT

Submitted by:
Florida Power Corporation

Written by:
B&W Nuclear Environmental Services
B&W Nuclear Technologies
Electric Power Research Institute
Florida Power Corporation
Packer Engineering

May 31, 1995

NOMENCLATURE

AVB-	Anti-Vibration Bar
AVT-	All Volatile Treatment
BWNT-	B&W Nuclear Technologies
BWOG-	B&W Owners Group
EC-	Eddy Current
EDS-	Energy Dispersive Spectroscopy
EPRI-	Electric Power Research Institute
FPC-	Florida Power Corporation
IGA-	Intergranular Attack
NDE-	Non-Destructive Examinations
OD-	Outside Diameter
OTSG-	Once-Through Steam Generator
POD-	Probability of Detection
RFEC-	Rotating Field Eddy Current
RPC-	Rotating Pancake Coil
RSG-	Recirculating Steam Generator
SAM-	Scanning Auger Microscopy
SEM-	Scanning Electron Microscopy
SG-	Steam Generator
TSP-	Tube Support Plate
TW-	Through-Wall
UT-	Ultrasonic Testing
WDS-	Wave Dispersive Spectroscopy
XPS-	X-ray Photoelectron Spectroscopy

TABLE OF CONTENTS

Section 1

BACKGROUND

1.1 Steam Generator Condition

Florida Power Corporation's (FPC) Crystal River-3 once-through steam generators (OTSGs) consistently exhibit minimal tube degradation due to either corrosion or mechanical damage. Six (6) tubes were plugged pre-service. Twenty-seven (27) tubes were plugged from 1978 - 1981 due to tube end/tube-to-tubesheet joint damage caused by a burnable poison rod assembly that broke loose and was transported to the upper bowl of the "B" SG by the primary coolant flow. The first time tubes were plugged due to in-service degradation was in 1987 when three (3) tubes were plugged in the "A" SG because of wear. By the end of 1989, a total of only 36 tubes had been plugged in the Crystal River-3 SGs. Currently, 182 (0.59%) of the total of 31,062 SG tubes at Crystal River-3 are plugged.

In 1989, FPC began to pro-actively inspect more SG tubes than the minimum number required by plant technical specifications. This increase in inspection scope was based both on industry guidelines, (i.e., EPRI Report NP-6201, PWR Steam Generator Examination Guidelines: Revision 2 which was issued December 1988 and recommended an inspection sample of 20% of the active tubes), and on the implementation of a more pro-active SG management philosophy. From 1989 - 1992, the population of tubes inspected was increased significantly to include more of the tubes that had not previously been inspected in-service. As a result of the 1989, 1990, 1992, and 1994 SG eddy current (EC) inspections, all active tubes in both SGs have been inspected at least once since 1987, i.e., 100% of the tubes have been inspected in seven (7) years (three fuel cycles).

Most of the tubes, however, had not been inspected in-service by EC since the pre-startup full-bundle inspection of the SGs. As the inspection scope increased, the number of EC indications increased, as well as the number of tubes plugged. The majority of these bobbin coil indications were below a 5:1 signal-to-noise ratio (S/N), and were in tubes that had no prior in-service EC inspection. Most of these EC indications were in the "B" SG. All of the tubes with EC indications (including low S/N indications) were re-inspected in subsequent outages to determine if they were growing. With the 1990 inspection results, concentrations of S/Ns in certain regions of the "B" SG became obvious. The regions with the highest number of S/N indications were the first span, 6" - 18" above the lower tubesheet secondary face (LTSF); the 7th tube support plate (TSP); and the 9th TSP (see Figures 1-1, 1-2, and 1-3). More than 90% of these indications have bobbin coil signals of less than 1 volt (see Figure 1-4).

Consistent with industry practice prior to 1992, FPC did not attempt to size any of

the S/N indications. All S/Ns were however tracked and re-inspected each outage to monitor for change in single amplitude. During this time it was not known whether S/Ns represented real degradation in the tube, or if they were caused by tube deposits. Further, because of the low signal-to-noise ratio, any real tube degradation could not be sized accurately by bobbin phase angle. Due to their small volume, the indications were not considered to be structurally significant even if they did have appreciable wall penetration. Therefore, leaving these indications in service was not considered a safety concern.

In 1992, however, industry practice began to change, and more focus was placed on trying to size S/Ns and disposition them according to the depth plugging criterion specified in plant technical specifications. FPC decided to pull tubes from the "B" SG during the Refuel 8 outage (in 1992) to determine if degradation was actually present where low S/N indications were being observed, to determine the probability of detection and accuracy in sizing of S/Ns by the available non-destructive examination (NDE) techniques, and to determine the structural significance of any degradation that might be present in the tubes.

The first span of the "B" SG had the most S/Ns, and afforded the highest potential for a successful tube pull due to the short length of tube that would require removal. Therefore, six (6) tubes with first span S/Ns were removed in June 1992. These tubes were cut just below the 2nd TSP and pulled from the bottom of the SG. A seventh tube with an EC indication at the 7th TSP was cut below the 8th TSP and its removal was attempted. However, it became stuck in the LTS before the area of interest could be removed. This tube was stabilized in place, and the tubesheet holes plugged.

These tubes were destructively examined in the laboratory by B&W Nuclear Technologies (BWNT) in collaboration with the Electric Power Research Institute (EPRI). The results of these examinations have been reported previously to the staff in Reference 1. A detailed description of the examinations and the results are documented in EPRI Report TR-103756, dated April 1994. These examinations revealed that real degradation was present in the tubes. The S/Ns were not caused by tube deposits. Small patches of pit-like intergranular attack (IGA) were present on the tubes. Burst testing showed that the pit-like IGA did not significantly lower the burst pressure of the tubes that were pulled.

Analysis of EC data showed that bobbin coil and rotating pancake coil (RPC) inspection techniques could not reliably detect this degradation type when the depth was less than 20% through-wall. The bobbin coil was found to have a probability of detection (POD) of 80% for a 45% or deeper through-wall IGA patch. The POD for RPC was somewhat less. It was further found that the pit-like IGA could not be accurately sized by bobbin coil phase angle.

Evaluation of the available historical EC data for the 1992 pulled tubes indicated that the pit-like IGA was present as early as 1980. No change in EC voltage has been observed since that time. The pit-like IGA inferred to be in other tubes, was determined by reviewing the historical EC data to have been dormant since at least 1989.

1.2 Purpose of 1994 Tube Pulls

Having determined the cause of the EC indications in the first span of the "B" SG, attention was turned to determining the cause of the EC indications at the 7th and 9th TSPs, the other large concentration of S/Ns in the "B" SG. FPC therefore decided to pull tubes with S/Ns at these locations in the 1994 Refuel 9 outage.

Other OTSGs also have varying numbers of low S/N indications. In 1993, the Steam Generator Committee of the B&W Owners Group (BWOG), began development of a pro-active tube pull program. The purpose of the program was to pull tubes with similar EC indications at similar elevations within the SGs from different plants in order to determine the cause of the indications, to determine their effect on tube structural integrity, and to determine the detection and sizing capabilities of a range of NDE techniques. This program would also aid in both the early identification of any degradation that might be active in OTSGs in general, and the development of preventative measures.

Based on a comparison of the quantity and location (elevation) of EC indications within each OTSG, the BWOG SG Committee recommended pulling at least four (4) tubes with EC indications in the 7th - 10th TSP region from the Crystal River-3B and Oconee-1B OTSGs in 1994, and Oconee-3 in 1995. The Crystal River-3 tube pull was thus incorporated into the BWOG program. Based on the results of this first phase of tube pulls, a determination would be made by the SG Committee whether additional tubes needed to be pulled. EPRI technical involvement was solicited by the SG Committee, and the tube pull program became a joint BWOG/EPRI collaborative program. The combined technical expertise of all five BWOG member utilities (i. e., Duke Power Company, Entergy Operations, GPU Nuclear, Toledo Edison, and Florida Power Corp.), B&W Nuclear Technologies, and EPRI was thus obtained for the tube pull program.

1.3 Rationale for Selection of Tubes Pulled

In May 1994, four (4) tubes were pulled from the Crystal River-3 "B" SG: 68-46, 72-49, 109-71, and 136-26 (see Figure 1-5). The criteria used to select the tubes to be pulled are listed below in order of priority:

(1) Adequate dome height to pull the tube.

(2) Multiple eddy current indications on the same tube. Within acceptable dome height, a maximum of two EC indications per tube was found in the 7th through 9th TSP region.

(3) Tubes with significant eddy current history. Over 2/3 of the tubes had been previously inspected only once (1992).

(4) Tubes with only one eddy current indication.

(5) Tubes which contained distorted tubesheet eddy current indications in the lower tubesheet.

Using the above criteria and the 1992 EC findings, eight (8) tubes were selected as candidates for pulling. From these eight candidates, four tubes were pulled based on their 1994 EC inspection results as described below.

Tube 68-46 had a distorted tubesheet signal at the LTSF; a low S/N indication at the 7th TSP; and a low S/N indication at the 9th TSP. This tube was inspected previously in 1992.

Tube 72-49 had a distorted tubesheet signal at the LTSF; a low S/N indication at the 7th TSP; and a low S/N indication at the 9th TSP. This tube was inspected previously in 1992.

Tube 109-71 had a low S/N indication at the 3rd TSP; and a 35% through-wall indication at the 7th TSP. This tube was inspected previously in 1992.

Tube 136-26 had a distorted tubesheet signal at the LTSF, and a 36% through wall EC indication at the 7th TSP. This tube was inspected previously in 1985, 1989, 1990, and 1992.

The four tubes were sent to BWNT for examination. This report summarizes the examinations performed and their results to date. Additionally, an archived tube, 41-44, from the 1992 tube pull was examined by BWNT. This tube contained low S/N indications in the first span, 6" - 18" above the LTSF, that were inferred to be pit-like IGA as observed in the other tubes pulled in 1992. The results from this tube are also included in this report.

Figure 1-1

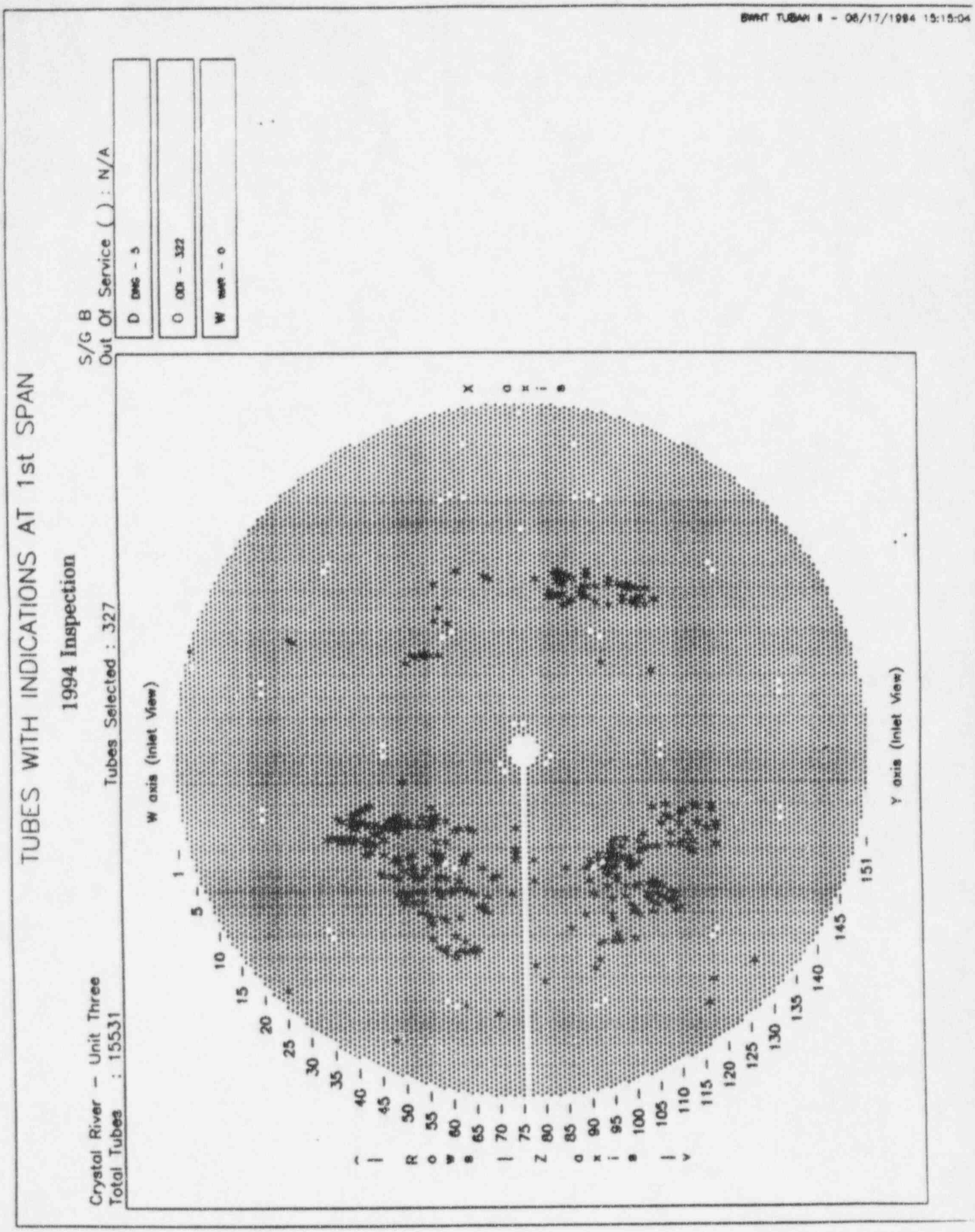
TUBES WITH INDICATIONS AT 1st SPAN
1994 Inspection
Crystal River – Unit Three
Total Tubes : 15531
Tubes Selected : 327
S/G B
Out Of Service ( ) : N/A
D DNG - 5
O ODI - 322
W axis (Inlet View)
Y axis (Inlet View)
X axis
Z axis

Figure 1-2

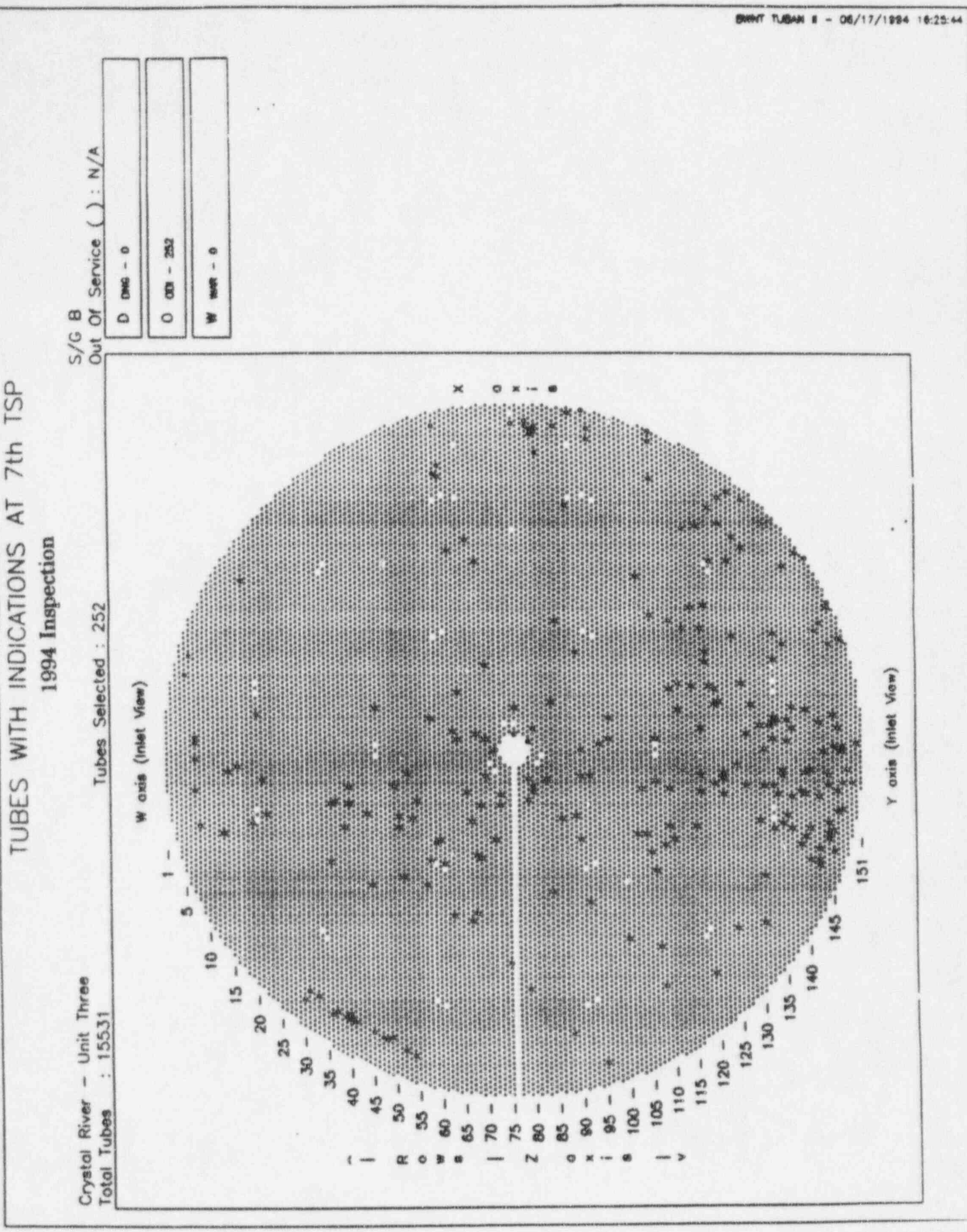
TUBES WITH INDICATIONS AT 7th TSP
1994 Inspection
Crystal River - Unit Three
Total Tubes : 15531
Tubes Selected : 252
S/G B
Out Of Service ( ) : N/A
D DNG - 0
O ODI - 252
W WAR - 0
W axis (Inlet View)
Y axis (Inlet View)
Rows
Z axis

VOLTAGE DISTRIBUTION - OVERALL

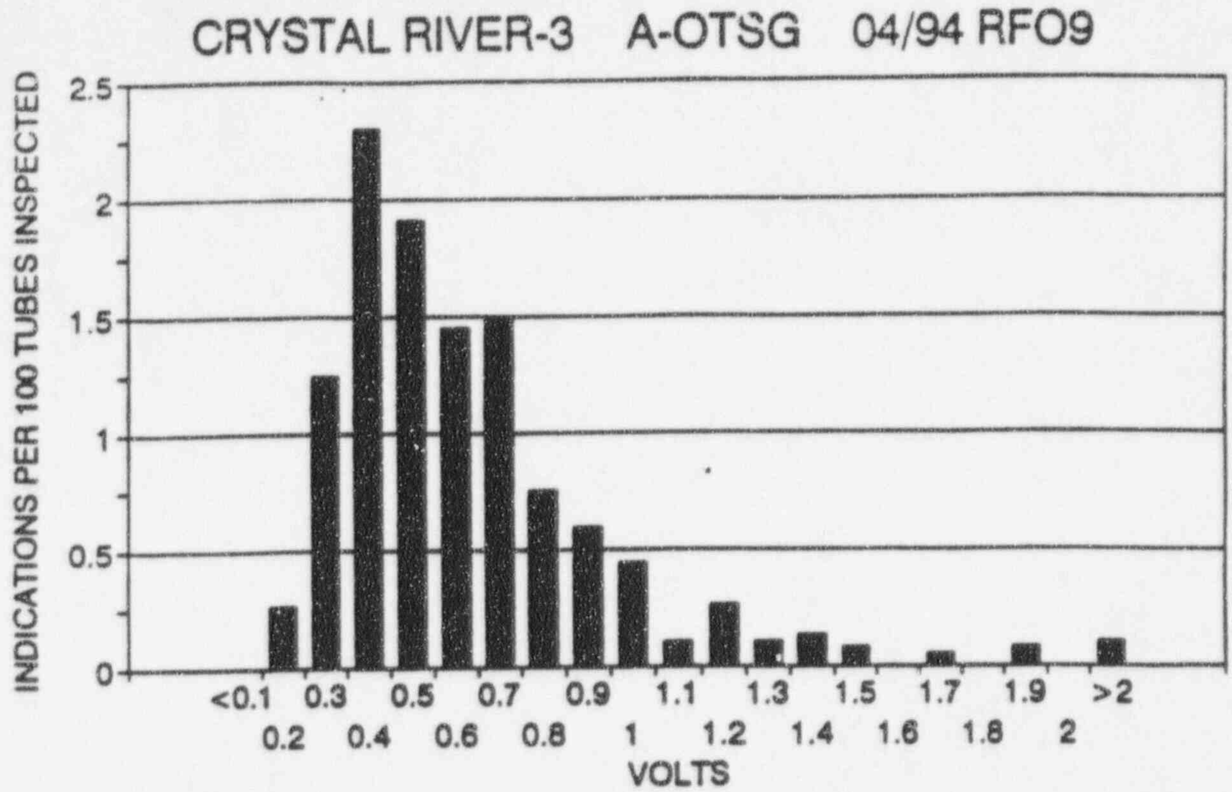

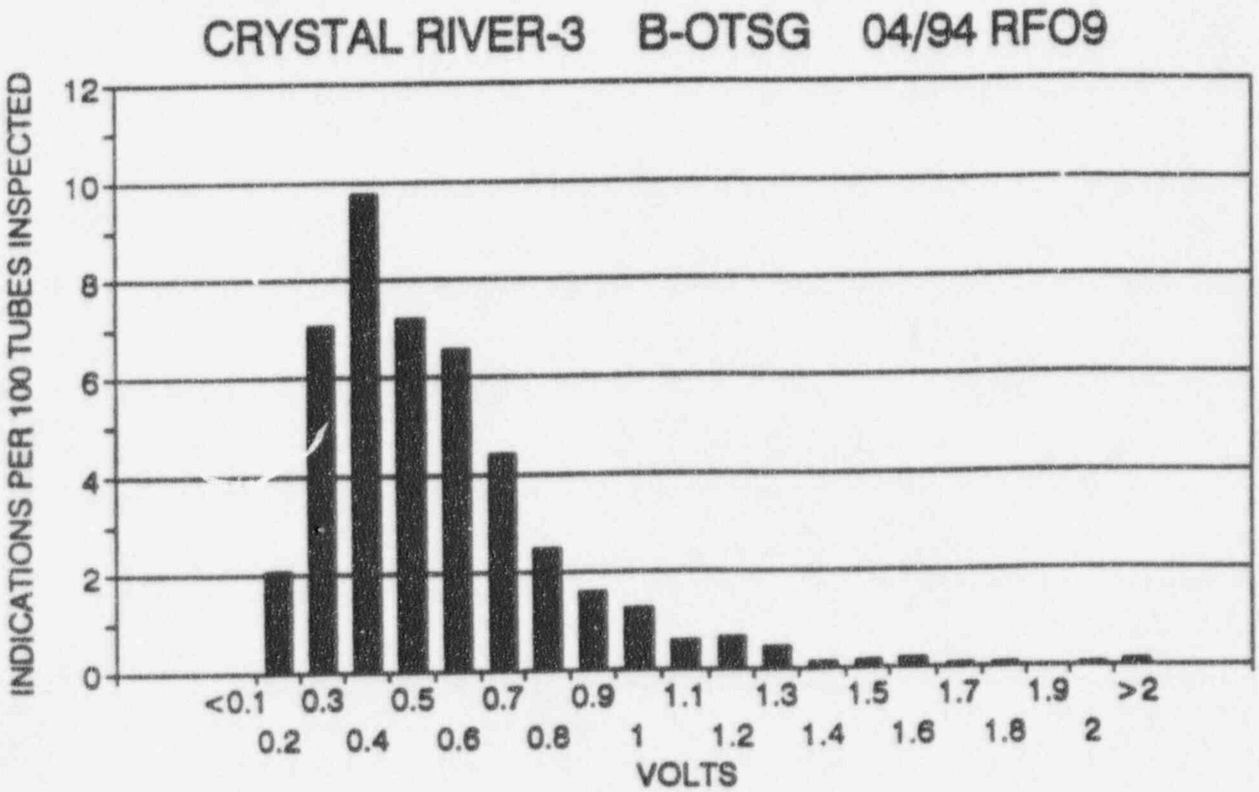

Figure 1-4

Figure 1-3

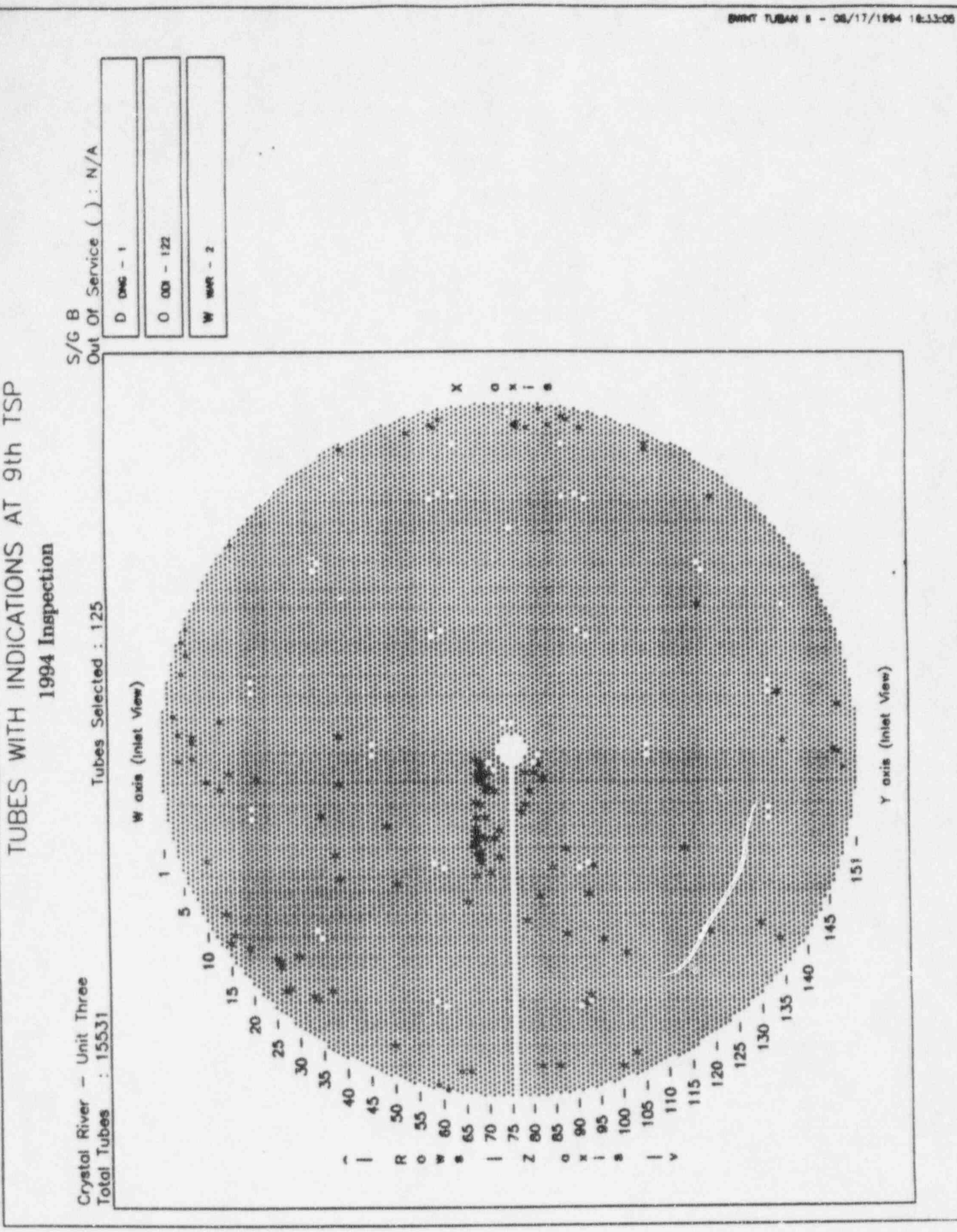
TUBES WITH INDICATIONS AT 9th TSP
1994 Inspection
Crystal River - Unit Three
Total Tubes : 15531
Tubes Selected : 125
S/G B
Out Of Service ( ) : N/A
D DNG - 1
O ODI - 122
W WAR - 2
W axis (Inlet View)
Y axis (Inlet View)
X axis
Rows - Z axis

TUBES PULLED 04/94 RFO 9

PLANT: CRYSTAL RIVER 3

GENERATOR: B

X = PULLED TUBE (4)

TOTAL TUBES : 15531

SUPPORT RODS ( ) : 48

TOTAL TUBES ASSIGNED : 4

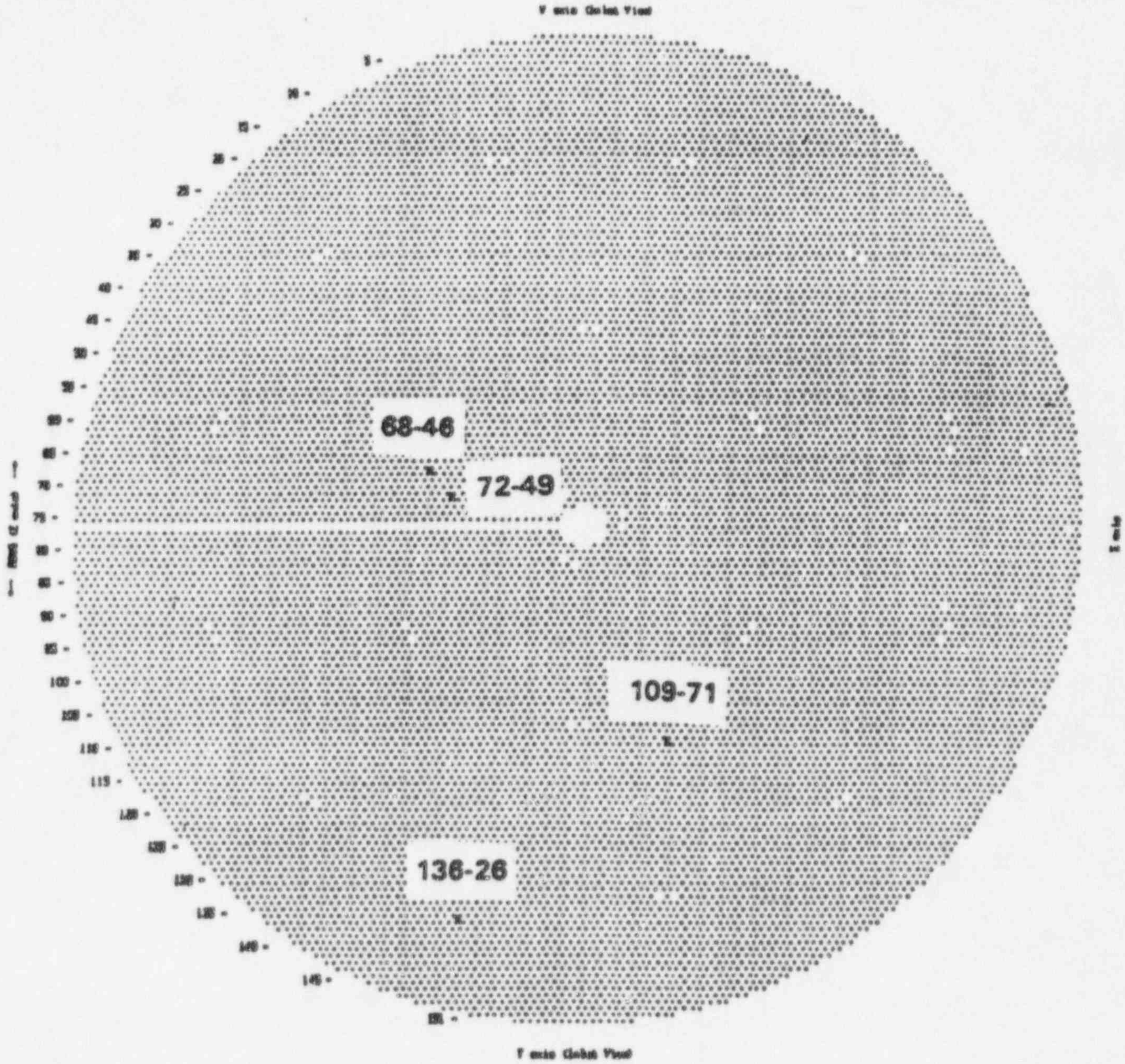

Figure 1-5

Section 2

EXAMINATION OF 1992 ARCHIVED TUBE AND 1994 PULLED TUBES

2.1 Field Nondestructive Examinations

A non-destructive examination (NDE) matrix was developed by the BWOG SG Committee for the field and laboratory inspections of the pulled tubes. This matrix was developed to complement the BWOG SG Committee Tube Integrity Project by investigating the probability of detection and accuracy in sizing of all NDE techniques and probes that can be used in OTSG size tubes. The Tube Integrity Project is a comprehensive program to determine at what size degradation in OTSGs become structurally significant, i.e. have unacceptably low burst pressures. The project will utilize machined and laboratory grown defects. The degradation that the BWOG Tube Integrity Project will investigate is wear, OD stress corrosion cracks, OD IGA, pitting, and dings (tube diameter distortions). These tube specimens will also be subjected to the same battery of NDE prior to burst testing as were the pulled tubes. Thus a comparison will be able to be made between the burst testing and NDE behavior of the machined and lab grown degradation to that in the field.

2.1.1 *Field NDE Test Matrix*

The pre-pull NDE matrix included extensive bobbin coil, rotating pancake coil (RPC), rotating field eddy current (RFEC), and ultrasonic testing (UT) probe examinations. The bobbin coil examinations utilized a 0.510" magnetic-bias universal long-cone, high-frequency (M/ULC/HF) and mid-frequency (M/UL/MF) probes; and a 0.540" high frequency (M/ULC/HF) and mid-frequency (M/UL/MF) probes. The test frequencies were 600, 400, 200, and 35 kHz in the differential and absolute modes. The RPC examinations utilized a 0.520" 3-coil, 0.80" diameter coil probe, and also a 0.115" diameter coil probe at frequencies of 300, 200, 100, and 10 kHz in the absolute mode. The RFEC examinations utilized a 0.510" probe at frequencies of 350, 200, 150 and 35 kHz in the absolute mode. All data was acquired and analyzed using Zetec's Eddynet system. The RFEC analysis used BWNT's EDDY-360 software. The examination of tubes by UT used a system called UT-360. The inspection involved sending the ultrasonic wave radially (zero degrees) in the tube wall. All RPC, RFEC, and UT was performed at 6" below to 6" above the LTSF, and at 2" above to 2" below the center of each TSP over the length of the tube section to be pulled. Each bobbin coil probe was run three (3) times full-length through each tube to study signal repeatability. Due to outage time restraints, UT was not performed in the field on tube 109-71.

2.2 Laboratory Nondestructive Examinations

The purpose of the nondestructive evaluations performed in the laboratory was twofold: (1) to confirm the field NDE indications and (2) to identify any additional

defect indications that were present. This was accomplished with extensive visual examination and photography, eddy current and ultrasonic inspections, radiography, and leak testing. Results of the nondestructive evaluation were also used in formulating the test plan for destructive evaluation of the tube segments. Results of the nondestructive evaluations are summarized in the following discussion.

2.2.1 *Laboratory NDE Test Matrix*

The post-pull NDE repeated a portion of the field ECT, but included more extensive UT than was performed in the field. The bobbin coil examinations utilized a 0.510" magnetic-bias universal long-cone, high-frequency (M/ULC/HF) probe on the four 1994 pulled tubes. The archived tube 41-44 was inspected with both the 0.510" M/ULC/HF and 0.540" M/ULC/HF probes. The test frequencies were 600, 400, 200, and 35 kHz in the differential and absolute modes. The RPC examinations utilized a 0.520" 3-coil, 0.80" diameter coil probe at frequencies of 300, 200, 100, and 10 kHz in the absolute mode. The RFEC examinations utilized a 0.510" probe at frequencies of 350, 200, 150 and 35 kHz in the absolute mode.

The examination of tubes by UT used the UT-360 system and included both zero degree and 45 degree shear wave examinations. The beam directions used in the examinations involved sending the ultrasonic waves radially (zero degrees) and circumferentially (45 degree circumferentially clockwise and counter-clockwise) in the tube wall.

Double wall radiography was also performed in the laboratory on those tube sections that had EC indications in the field.

The laboratory NDE test matrix is shown in Table 2-1.

2.3 NDE Test Results

The pre and post-pull NDE of both the Crystal River-3 and Oconee-1 pulled tubes was performed as a BWOG SG Committee project. A comparison of the NDE results to the tube metallography results from both plants will be performed later as a BWOG project. A detailed comparison of the 0.510" HF bobbin coil and the 3-coil 0.080" diameter coil MRPC data to the destructive examination results has been performed to determine the probability of detection and accuracy in sizing of each probe/technique. The accuracy in sizing of these two probes as well as the measurement repeatability of the 0.510" bobbin coil are discussed in Reference 14 and is not repeated here. The probability of detection for these two probes are discussed in this section. The capabilities of UT, RFEC, and the 3-coil 0.115" diameter coil MRPC will be evaluated later as a BWOG project. In summary, the results of the non-destructive examinations are as follows:

1. No visual evidence of corrosion was found during the nondestructive evaluation.

2. Laboratory and field EC techniques agreed in most cases, with the following exceptions:

   - Eddy current distorted tubesheet signals at the lower tubesheet secondary face were not seen by EC in the laboratory, thus these signals do not appear to be connected with any tube degradation.

   - Consistent with the 1992 pulled tube examinations, several volumetric indications were found in the lower tubesheet crevice region of tubes number 68-46 and 72-49 which were not detected in the field eddy current examinations.

3. Most defect indications that were found by EC appear to correlate both visually and radiographically with "wear" marks at the broached tube support plate "lands".

   - At the 7th TSP, circular or "D"-shaped wear marks were observed at the bottom edge of the lands on all four pulled tubes. Figure 2-1 is an example of this type of defect.

   - At the 9th TSP, "tapered" wear marks (see Figure 2-2) were observed at the top edge of one TSP land <u>and</u> the bottom edge of a second, adjacent TSP land. These marks were axial in orientation and deepest at the edge of the support plates.

4. Spots of yellow deposit "nodules", as shown in Figure 2-3, were observed, most predominantly within the lower tubesheet crevice regions and first (lowermost) tube span of tubes 68-46 and 72-49. Streaks of white deposit were also observed in the upper elevations (Figure 2-4) on all four 1994 pulled tubes.

5. No through-wall penetrations were found to be associated with any of the defect indications, as confirmed by helium leak test.

In general, for all laboratory eddy current examination techniques, the majority of the indications reported in the field were confirmed in the laboratory. Discrepancies in voltage and additional calls in the laboratory were the result of the effect of TSPs or tubesheet on the signals analyzed in the field. No new or different modes of degradation were detected.

2.3.1 *Probability of Detection*

The probabilities of detection (POD) of both the bobbin coil and MRPC versus the depth of pit-like IGA observed by metallography in four (4) 1992 pulled tubes was presented in Reference 3. The 0.510" high frequency bobbin coil probe was used both in the field and laboratory inspections of the 1992 pulled tubes. The test frequencies were 600, 400, 200, and 35 khz in the differential and absolute modes. The MRPC inspections utilized a 0.520" 3-coil, 0.080" diameter coil probe. The probability of detection of each technique versus the depth of the discontinuity as determined by metallography was shown graphically in the aforementioned reference. The 1992 POD graphs, however, combined both the field and laboratory eddy current inspection results, giving higher PODs than that experienced in the field.

The 1994 pulled tubes were inspected prior to pulling by the same type bobbin coil and MRPC probe as was employed in the 1992 inspections. As with the 1992 pulled tubes, the length, depth, and width of the discontinuities in the 1994 pulled tubes as well as one 1992 archived tube were determined by metallography. The 1994 and 1992 archived pulled tube data (16 data points) was combined with the previous 1992 pulled tube data (67 data points), and new POD graphs were constructed. Only field eddy current data was used. Only discontinuities which had been examined by metallography to determine its length, width, and depth were used to develop POD relationships. Due to the active bobbin coil area having an axial extent of around 0.200 inch, any multiple discontinuities found by metallurgical examination that were less than 0.200 inch apart were combined as one flaw for comparison. Because the probability of detection can vary based on discontinuity morphology, and location within the steam generator (e.g., tubesheet, freespan, tube support plate (TSP)), the probability of detection was evaluated separately for each of the following three cases: (1) pit-like IGA inside the lower tubesheet (LTS); (2) tapered wear at the TSP, and (3) volumetric discontinuities (i.e., pit-like IGA and circular wear) outside of the tubesheet.

2.3.1.1 *Probability of Detection in the Lower Tubesheet*

Sixteen (16) IGA patches that were present in the lower tubesheet portion of four pulled tubes were destructively examined to determine the dimensions of the degradation. Two (2) of the IGA patches, including the largest through wall patch, were in the 1994 pulled tubes. Eleven (11) of the IGA patches were 20% or less through wall in depth; four (4) were 21 -40% through wall; and one IGA patch was 75% though wall at its deepest penetration. The axial length of all but one of the IGA patches was less than 0.074 inch. The deepest IGA patch also had the longest length, 0.228 inch. None of these discontinuities were detected in the field by either bobbin coil or MRPC eddy current.

The 75% TW IGA patch present in the LTS of 68-46 was detected by eddy current in

the laboratory. Its location corresponded to large amplitude volumetric indications found during laboratory eddy current inspection by both bobbin and RPC. This large amplitude signal condition was not observed during field examinations where instead a small amplitude, low signal-to-noise ratio, signal was observed. The increase in voltage observed in the laboratory exam is due, presumably, to trauma experienced by the tube during removal operations (cutting, pulling, shipping, etc.). Metallography determined the degradation to be similar to the pit-like IGA that was present in the first span and lower tubesheet region of tubes pulled in 1992, although the axial length is greater.

2.3.1.2 *Probability of Detection of Tapered Wear*

Four (4) tapered wear scars present on two tubes pulled in 1994 were examined in the laboratory. The maximum depth observed in any of the scars was less than 20% through wall. The lengths of the scars were up to 0.64 inch. All four tapered wear scars were detected by both bobbin coil and MRPC eddy current inspection.

2.3.1.3 *Probability of Detection of Non-Tubesheet Volumetric Discontinuities*

Sixty-seven (67) eddy current distinguishable non-tubesheet, volumetric discontinuities (i.e., greater than 0.200 inch apart) were subjected to metallurgical examination. These discontinuities consisted of five (5) circular wear scars, and 62 pit-like IGA patches. All five (5) circular wear scars were from the 1994 pulled tubes. Nine (9) of the IGA patches were from the 1992 archived tube that was destructively examined in 1994. The probability of detection was found to increase as the axial length and/or volume of the discontinuity increases as shown in Figures 2-8 and 2-9, respectively. The distribution of axial lengths observed in the 1992 and 1994 pulled tubes is shown in Figure 2-10. All of the IGA patches had lengths of 0.074 inch or less. All of the discontinuities with axial extents longer than 0.074 inch were circular wear.

The findings of Figures 2-8 and 2-9 are consistent with the expectation that the probability of detection increases as the degradation increases in size. Figure 2-8 and 2-9 also show that both the 0.510" bobbin coil and the 0.080" diameter coil 3-coil MRPC have generally about the same detection probability.

The 0.540" HF bobbin coil exhibited slightly better detection performance than the 0.510" HF bobbin coil, detecting two additional discontinuities (an IGA patch and a small tapered wear scar) in the 1994 pulled tubes. Generally, the 0.540" HF bobbin coil data was cleaner (higher signal-to-noise ratio) and more repeatable than the 0.510" HF bobbin coil. Since the 1994 pulled tubes contained fewer indications than the 1992 pulled tubes, only about 11 indications were detected by the 0.540" HF bobbin coil. This number is indications is too small to make any quantitative assessment of the capabilities of the 0.540" probe.

2.4 Destructive Examinations

Based on the nondestructive examination results, a detailed test plan was formulated for the destructive examination, as shown in the Task 2 matrix of Table 2-1. The objectives of the destructive examinations carried out were to (1) verify base tubing material properties, (2) establish the damage mechanism for any degradation identified, (3) establish correlations between tube condition and EC signals, especially low S/N indications, (4) determine the effect of degradation on the burst strength of the tubing, and (5) determine the thickness, morphology, and chemical composition of any deposits present on the tube OD surfaces. All of the analyses have been completed with the results summarized in the following discussion. All of the results will be presented in the final report to EPRI, scheduled for completion in 1995.

2.4.1 *Defect Evaluation*

Destructive examinations were carried out on tube sections with defect indications and included deposit collection and chemical analysis, tube swelling to facilitate deposit collection and/or to open up small defects for sectioning, burst testing to characterize the effect of tubewall degradation on burst pressures, defect metallography and fractography, and base metal characterization.

2.4.1.1 *Burst testing*

Burst testing was conducted to determine the effect of the observed degradation on the pressure-holding capacity of the tubes and to open up any intergranular degradation that might be present. Burst testing was performed in strict accordance with industry guidelines established by EPRI (see Reference 2) for steam generator tubes. For baseline comparisons, one defect-free section from each of the pulled tubes, including archived tube numbers 41-44, 97-91, and 106-32, was also tested. Results are shown in Table 2-2.

During expansion of a section of tube number 68-46 from the lower tubesheet region for collecting deposits, a leak developed at ~6914 psi at an elevation ~0.6 inch below the secondary face of the tubesheet. The tube was then shimmed and the actual burst pressure per EPRI guidelines was obtained, as shown in Table 2-2. The IGA patch at which rupture occurred (see Figure 2-5) was about 0.23" in length (axial) and ~70% through wall. Its location corresponded to large amplitude volumetric indications found during laboratory eddy current inspection by both bobbin and RPC. This large amplitude signal condition was not observed during field examinations where instead a small amplitude low signal-to-noise ratio was observed. The increase in voltage observed in the laboratory exam is due, presumably, to trauma experienced by the tube during removal operations (cutting, pulling, shipping, etc.). Metallography determined the degradation to be similar to the pit-like IGA that was present in the first span and lower tubesheet region of tubes pulled in 1992, although the axial

length is greater.

Defect-free sections of archived tubes 97-91 and 106-32 were also tested for comparison with burst pressures obtained during the previous tube pull (see Reference 3). In both cases, the defect-free burst pressure was less than the burst pressures obtained in 1992 for sections having pit-like IGA. The reason for the discrepancy has been determined to be a result of error introduced by the higher rate of pressurization used in the 1992 tests (prior to the issuance of standardized test procedures by EPRI). The discrepancy is explained in detail in Appendix A, along with corrections applied to the previous data.

As can be seen in Table 2-2, the effect of the observed tubewall degradation on burst pressure is minimal with the exception of the IGA patch on tube number 68-46. However, as discussed in Section 3.2, no structural margins were exceeded in any of the tubes because of the degradation present.

2.4.1.2 *Defect Metallography*

Extensive metallography was carried out on selected tube sections to obtain dimensional information (extent and depth) and to confirm the presence or absence of degradation. Results are summarized in Table 2-3 (detailed results will be presented in the final EPRI report).

For archived tube number 41-44, a total of 33 patches of pit-like IGA were found in the first span section, in a band from 5 to 19 inches above the secondary face of the lower tubesheet (Figure 2-6). Typically, these patches were ~30% through wall and similar in size to those seen in the other tube sections removed in 1992. Burst occurred at a defect ~50% through wall. The location and morphology of these defects are identical to those found in other tubes removed from Crystal River-3 in 1992.

For the pit-like IGA defects found in the lower tubesheet crevice regions on tube numbers 68-46 and 72-49, strong sulfur peaks were noted on all grain faces and on adjacent deposits by energy dispersive spectrometer/wave dispersive spectrometer (EDS/WDS) analysis. This would suggest that the corrosion mechanism is similar both to that reported previously in Reference 3, and, to that found also on tube number 41-44 as noted above; i.e., reduced-sulfur IGA.

The wear marks observed at the tube support plate edges appear to be simple mechanical wear. No conclusive evidence of corrosion was found associated with these defects.

2.4.2 *Deposit Analysis*

In general, the tube OD surfaces were covered with a thin, tenacious layer of black

deposit. First span regions exhibited a "mottled" appearance, similar to the tubes pulled during in 1992. Tube support plate land contact areas were easily seen due to the general absence of deposit at the contact area. In some cases, the flow patterns through the support plate broaches were clearly visible as the result of differences in deposit buildup and color. Deposit loading increased with elevation, reaching a maximum of ~0.34 grams/inch (2.25 mils thick) at approximately the 6th TSP elevation and decreasing rapidly above this elevation (Figure 2-7). This pattern of deposit loading is typical for once through steam generators which reach dryout at about mid-length in the bundle.

In the lower tubesheet crevice regions, which are relatively free of deposit, yellow deposit nodules (Figure 2-3) were observed. EDS/WDS analysis confirmed that this deposit is elemental sulfur.

In the upper elevations, white streaks of deposit were observed. Scanning electron microscope (SEM)/EDS/WDS analysis suggests that this deposit is thin, relatively fine-grained and rich in manganese and other hardness contaminants. The thin streaks are deposited on top of the magnetite deposits on the tube.

Samples of OD deposits were removed from regions of degradation and from the free span areas at several elevations for chemical analysis, for deposit loading, and for density and porosity determination. Results indicate that the deposit is primarily magnetite, which typically forms on boiling surfaces in steam generators using all volatile treatment (AVT) water chemistry control. Detailed results of the chemical analysis of the deposits will be included in the final EPRI report.

2.4.3 *Material Properties*

Material properties were determined for each of the four pulled tubes and for the archived tube number 41-44. Results are tabulated in Table 2-4. All material properties are typical of sensitized OTSG tubing; nothing unusual was noted.

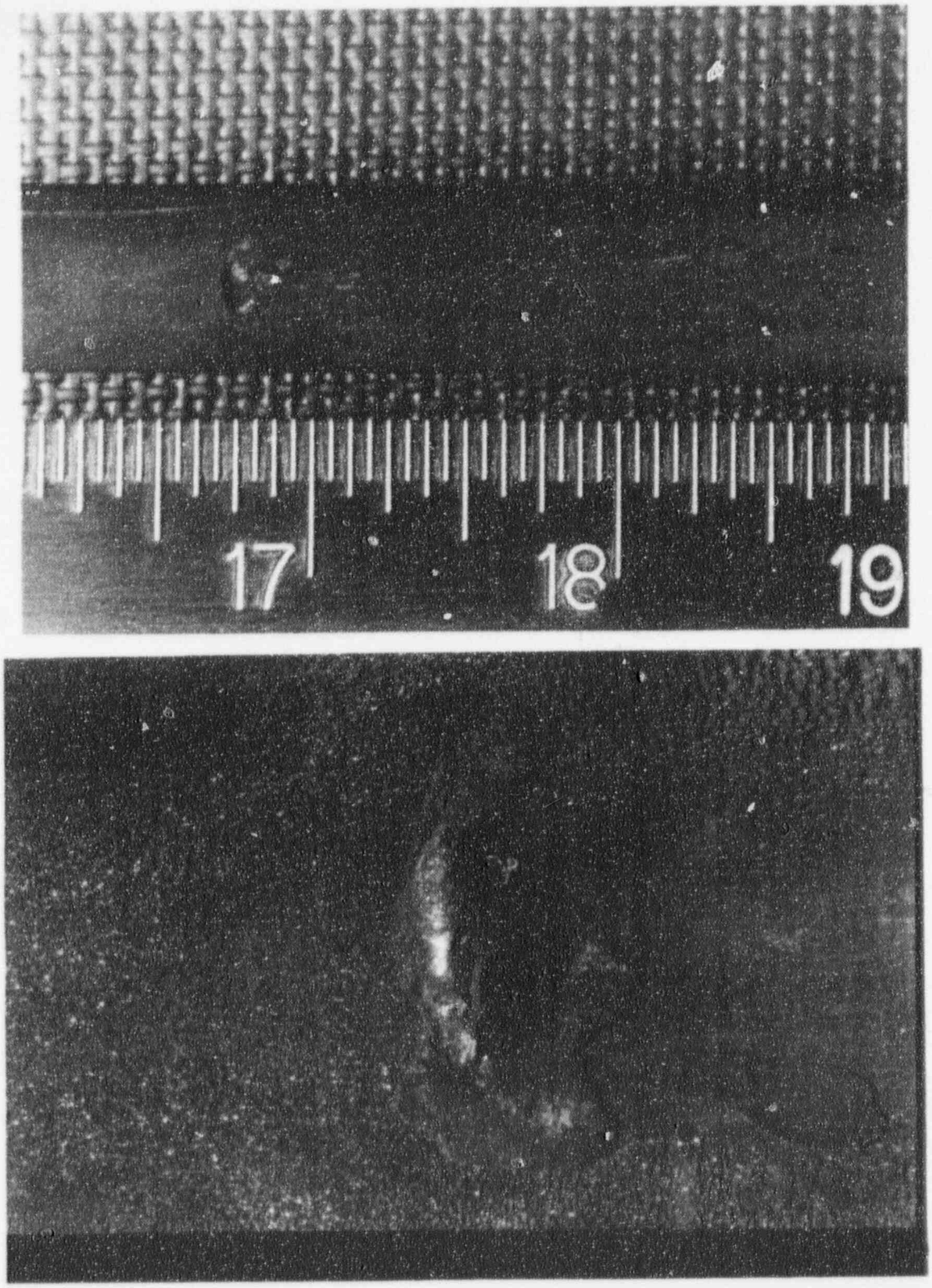

Tube Section 136-26-15
Wear Mark at 7th TSP

Figure 2-1

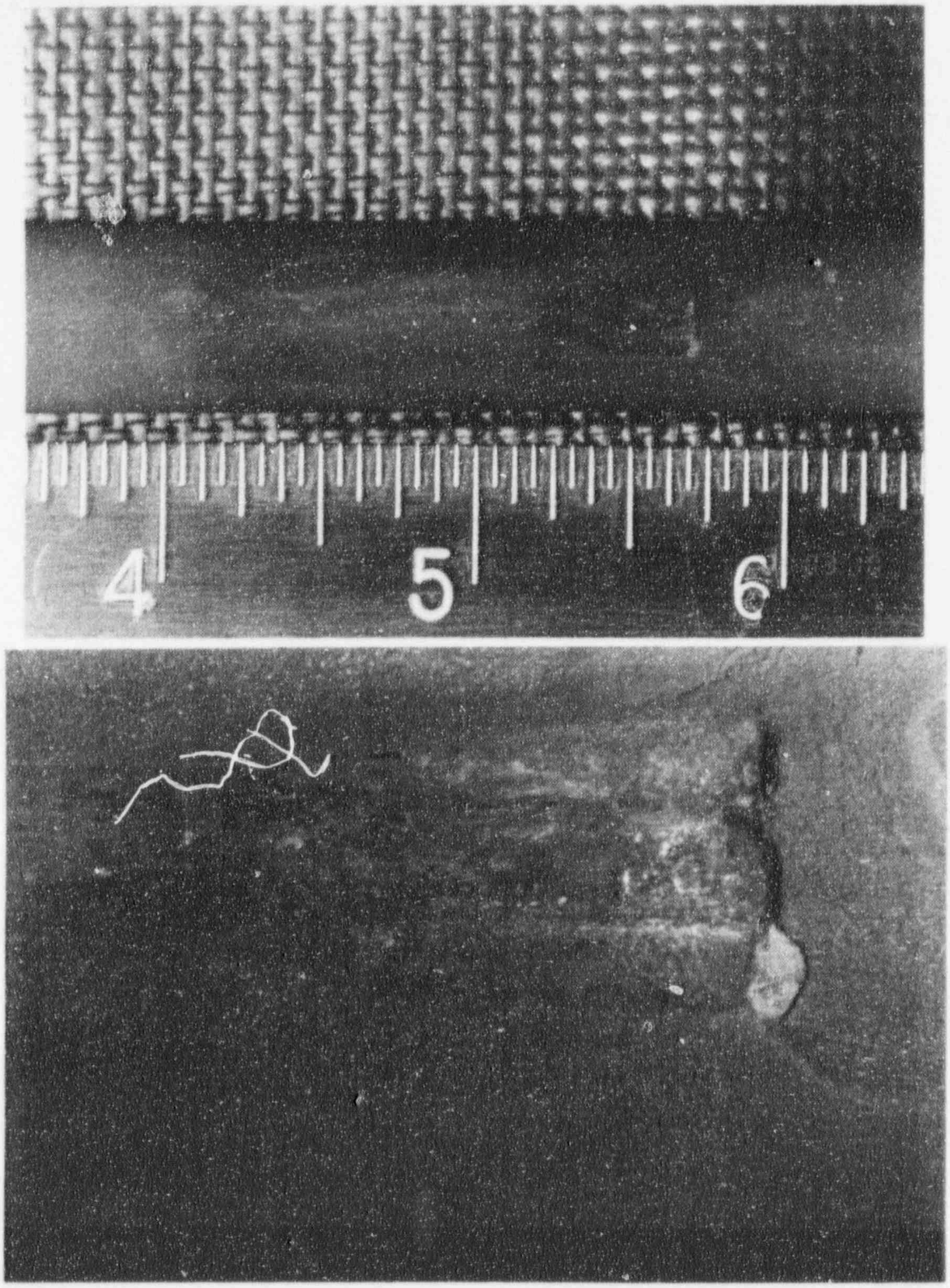

Tube Section 68-46-18
Tapered Wear Mark at 9th TSP

Figure 2-2

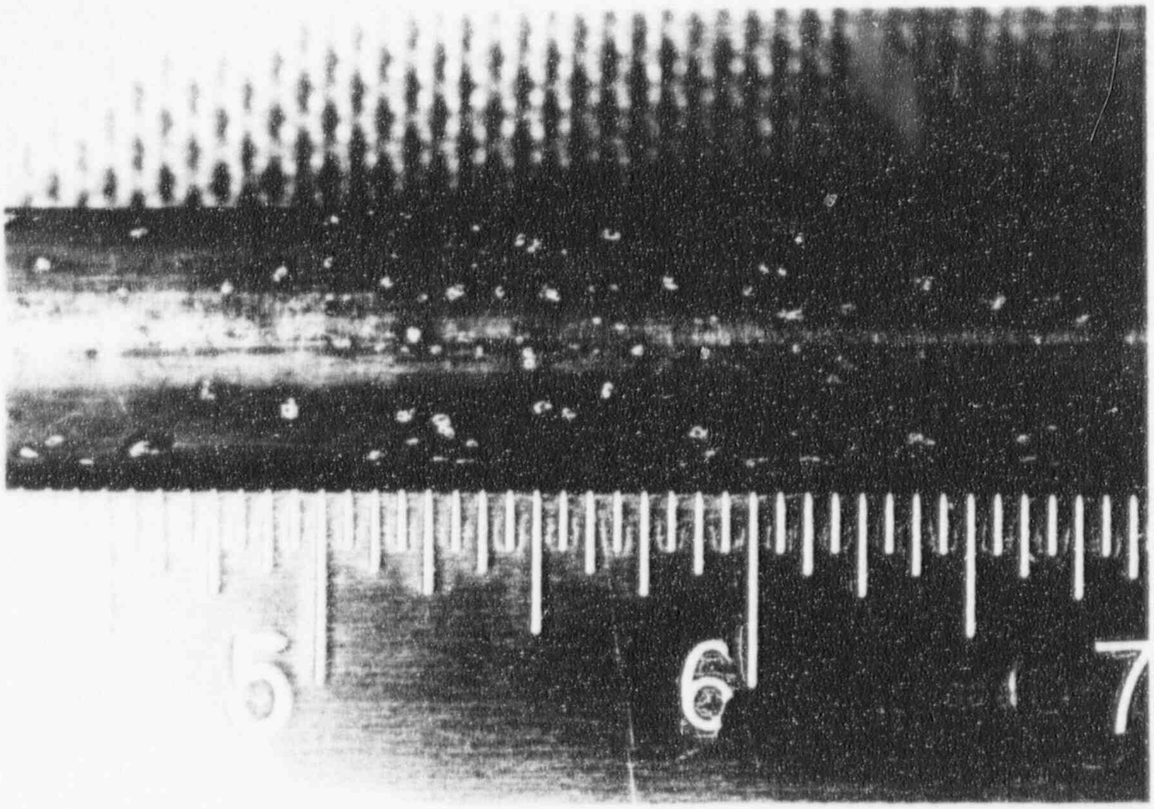

YELLOW DEPOSIT IN LOWER TUBESHEET CREVICE

Figure 2-3

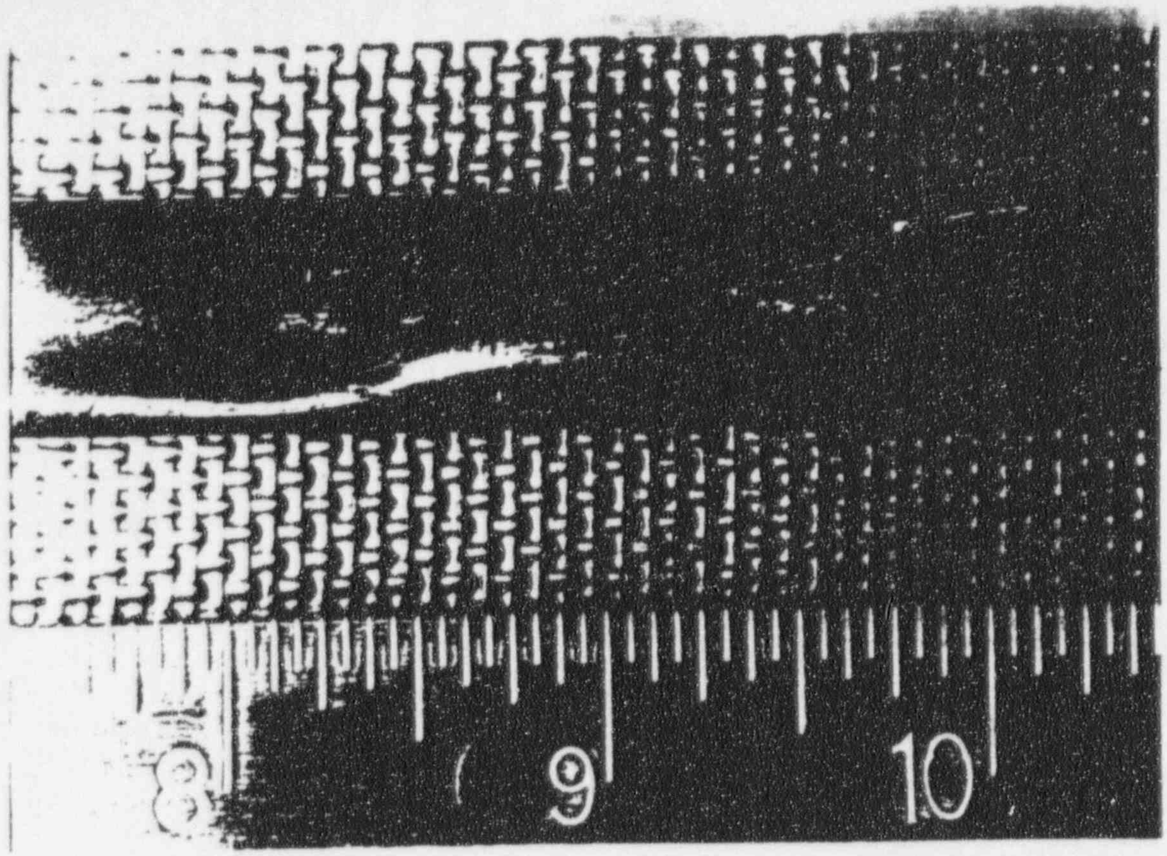

TYPICAL STREAK OF WHITE DEPOSIT AT TSP (TUBE 68-46-20)

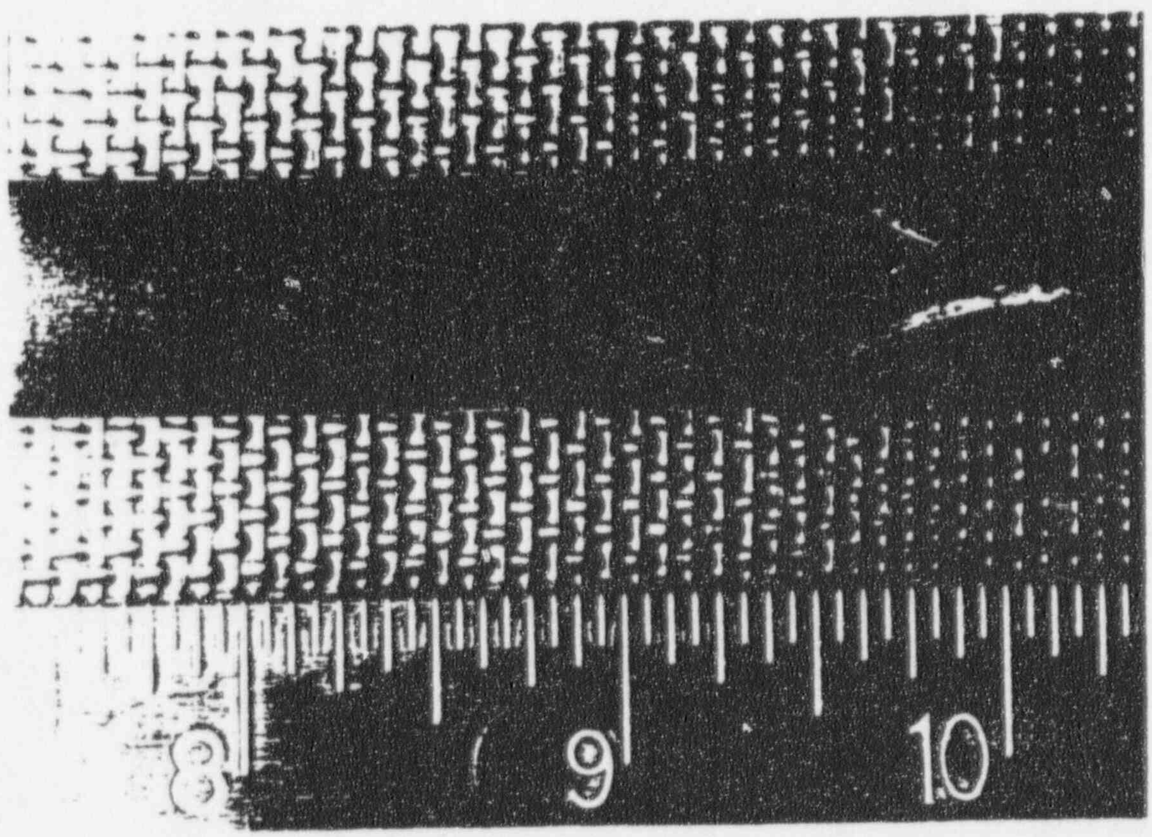

Figure 2-4

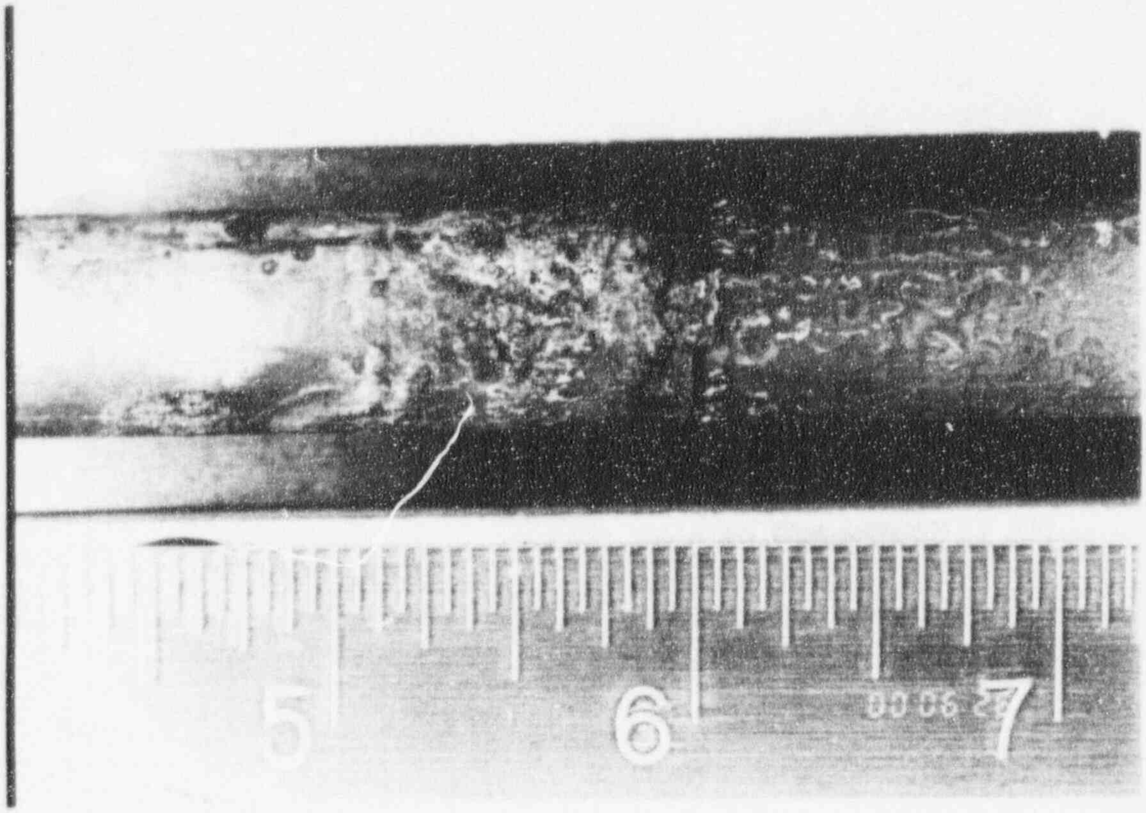

INTERGRANULAR DEFECT ~½-IN. BELOW TTS (TUBE 68-46-3)

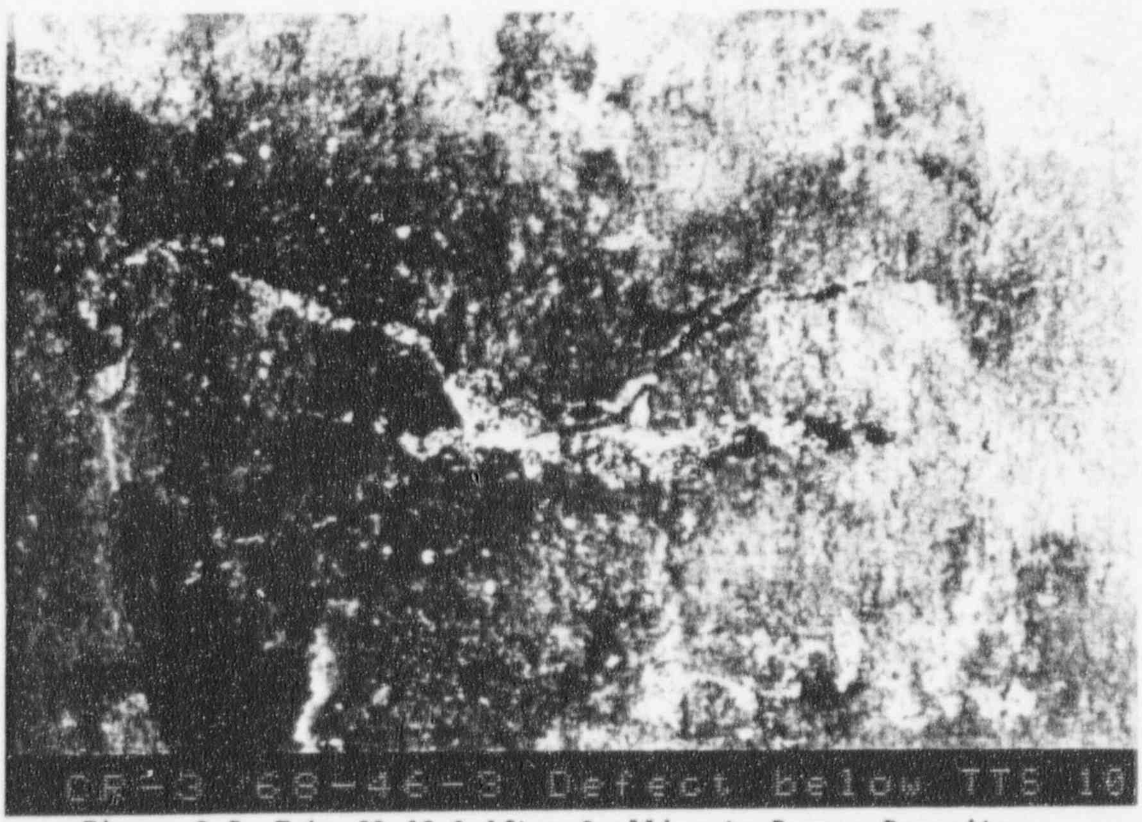

Figure 2-5. Tube 68-46-3 After Swelling to Remove Deposits.

Figure 2-6

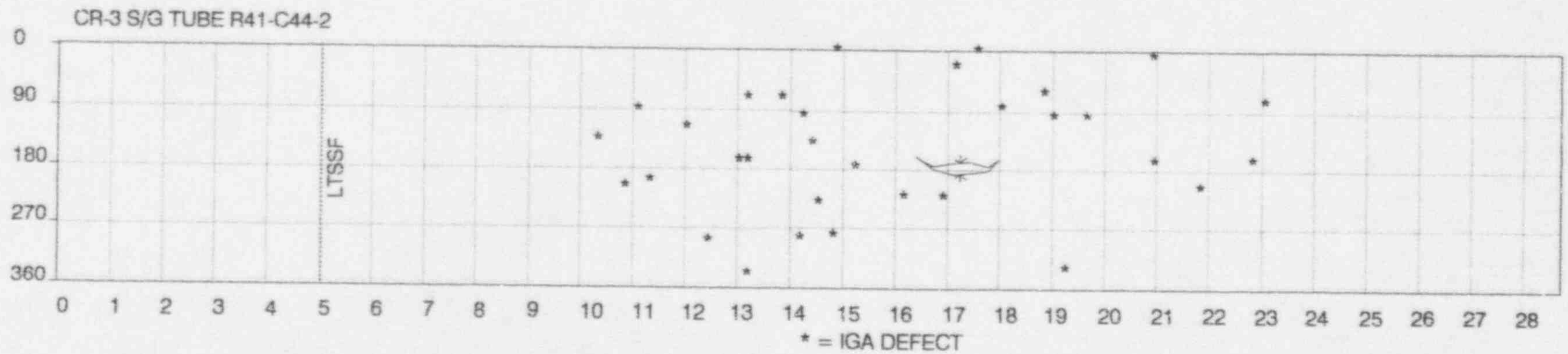

Tube Section 41-44-2
Map of discovered small IGA patches

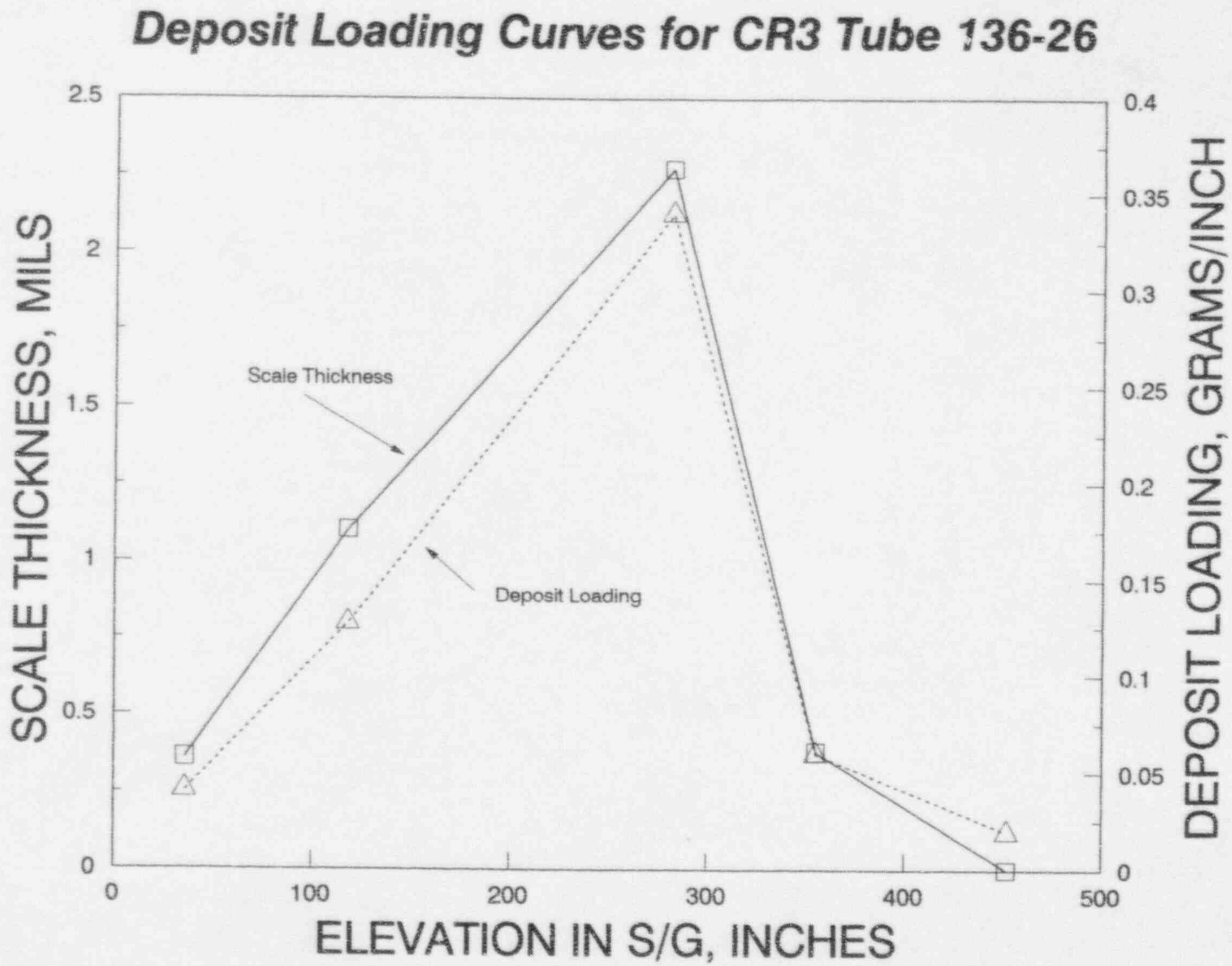
Deposit Loading Curves for CR3 Tube 136-26
SCALE THICKNESS, MILS
DEPOSIT LOADING, GRAMS/INCH
ELEVATION IN S/G, INCHES
Scale Thickness
Deposit Loading
0
0.5
1
1.5
2
2.5
0.05
0.1
0.15
0.2
0.25
0.3
0.35
0.4
100
200
300
400
500

Figure 2-7

Figure 2-8. Crystal River-3 Field Eddy Current Detectability vs. Axial Length for Non-Tubsheet Defects in the 1992 & 1994 Pulled Tubes

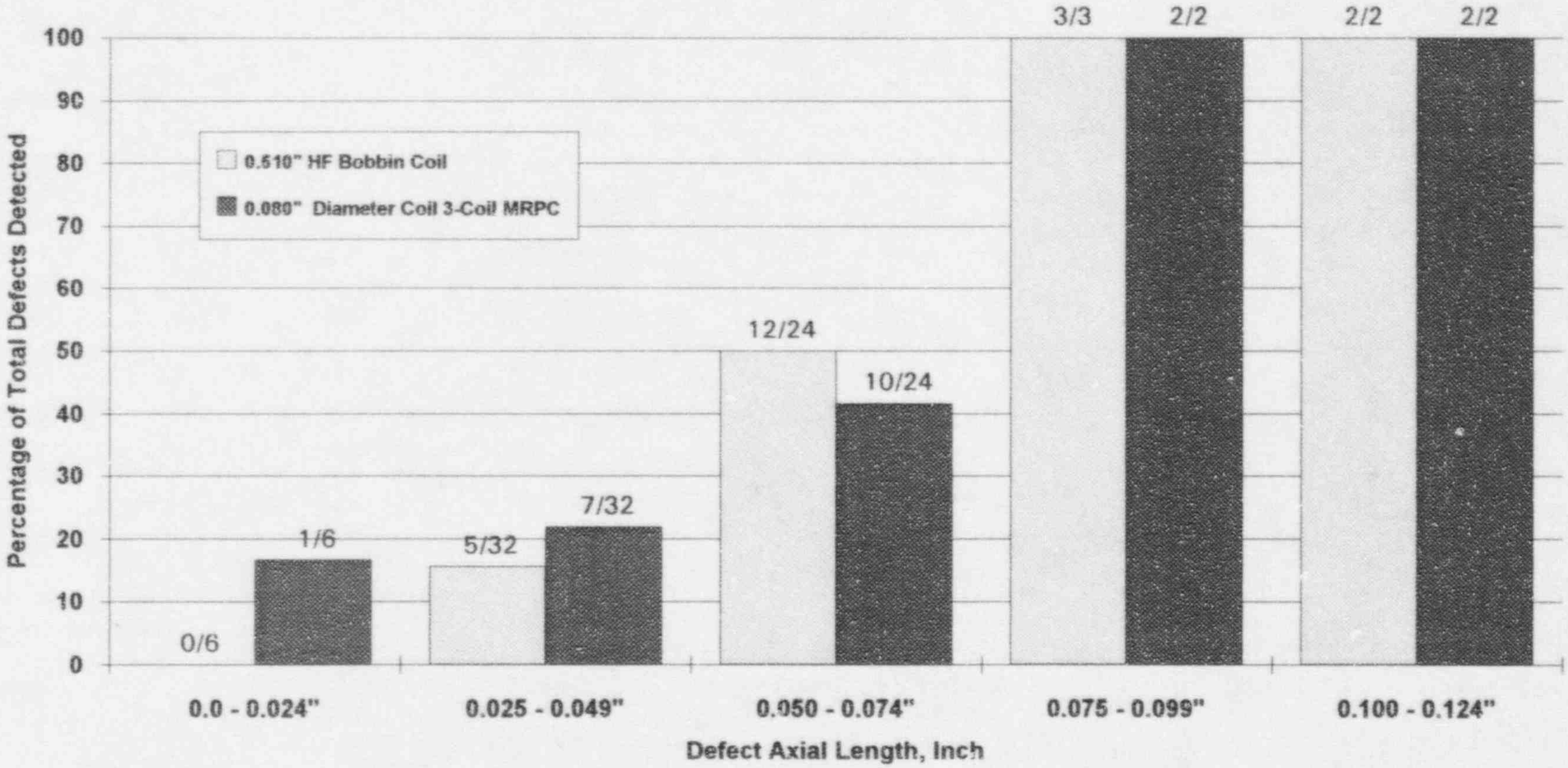

Figure 2-9. Crystal River-3 Field Eddy Current Detectability vs. Volume for Non-Tubesheet Volumetric Indications in the 1992 and 1994 Pulled Tubes

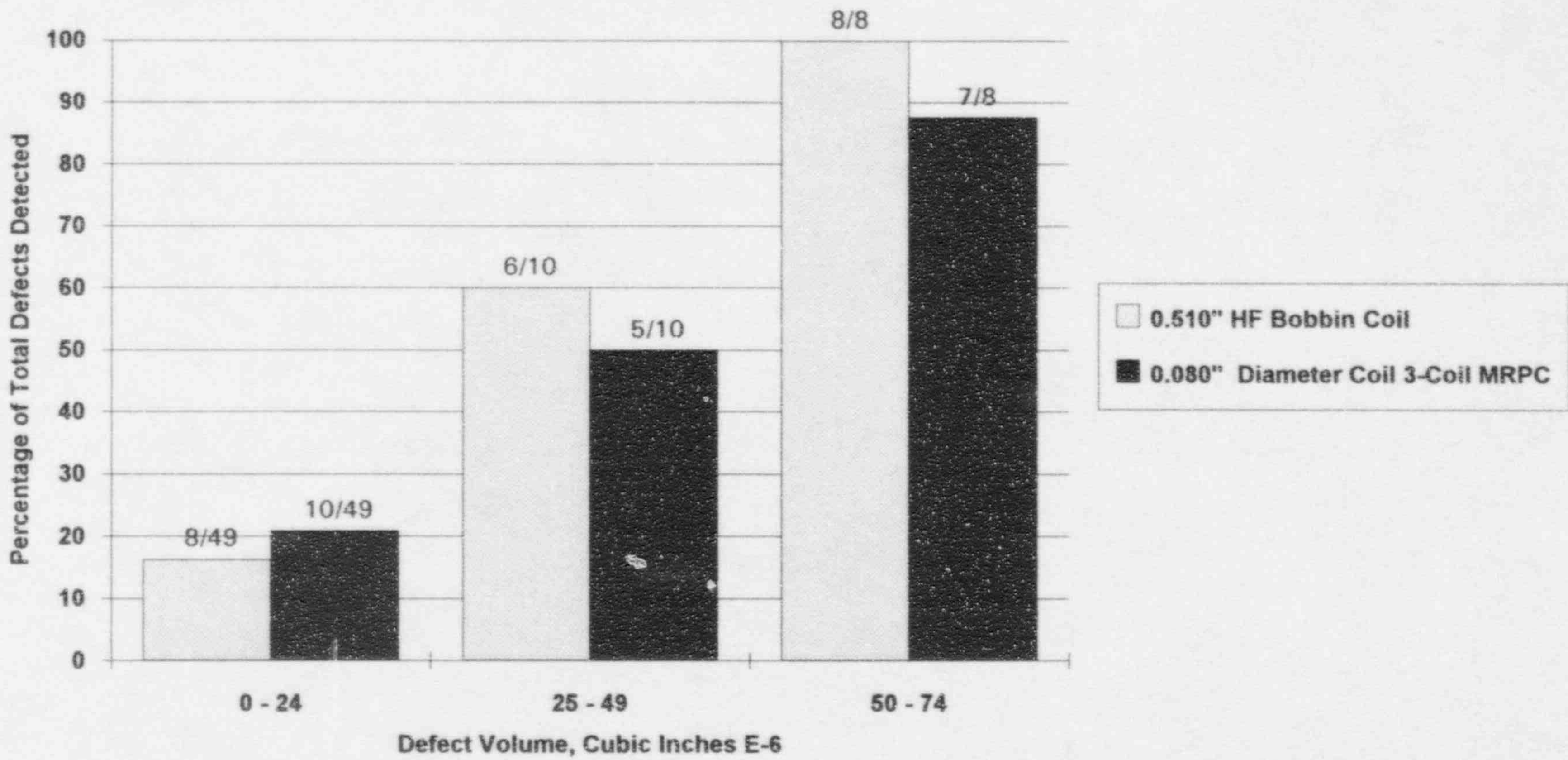

Figure 2-10. Axial Length Distribution of the Non-Tubesheet Discontinuities from the 1992 & 1994 Crystal River-3 Pulled Tubes

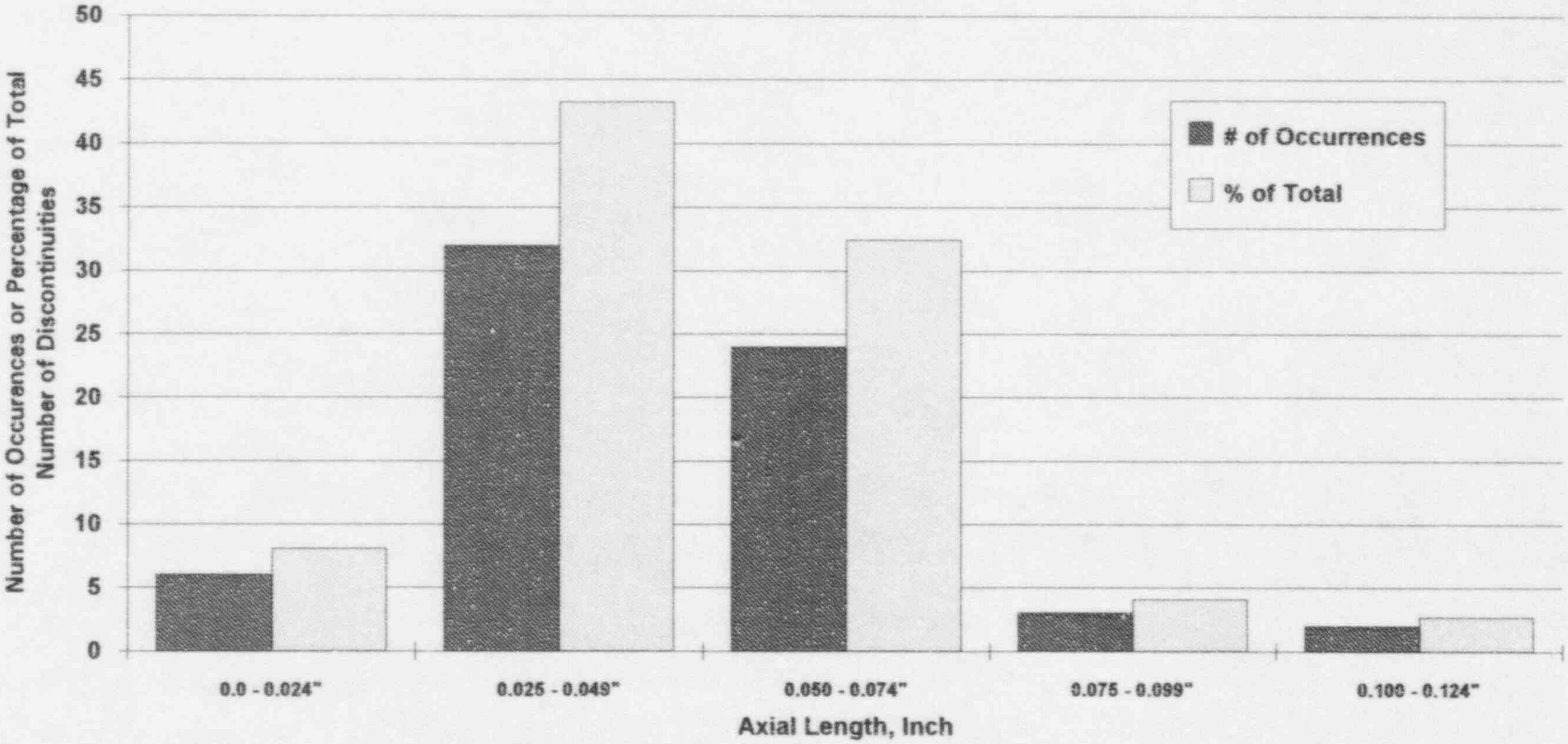

Table 2-1
Nondestructive Scope

Receipt Inspections	All Sections
Visual Inspections (Photography)	All Sections; photograph tube 136-26 in one orientation full length.
Bobbin Coil ECT	All Sections

	68-46					72-48					109-71		136-26			41-44
	1	2	3	14	18	2	5	7	13	17	7	14	2	9	15	2
	LTS	LTS	LTSF	7th TSP	9th TSP	LTSF	2nd TSP	3rd TSP	7th TSP	9th TSP	3rd TSP	7th TSP	LTSF	3rd TSP	7th TSP	LTSF
	NDD	NDD	IGA	Wear	Wear	IGA	NDD	NDD	Wear	Wear	Wear	Wear	NDD	NDD	Wear	IGA
Stpereovisual Inspections, *	Y	Y	Y	Y	Y	Y	Y	Y	Y	Y	Y	Y	Y	Y	Y	Y
MRPC ECT			Y	Y	Y	Y		Y	Y	Y	Y	Y	Y		Y	Y
Rotating Field ECT			Y	Y	Y	Y	Y	Y	Y	Y	Y	Y	Y	Y	Y	Y
Ultrasonics Testing			Y	Y	Y	Y			Y	Y	Y	Y	Y		Y	
X-Ray Radiography			Y	Y	Y	Y	Y	Y	Y	Y	Y	Y	Y	Y	Y	Y
Helium Leak Test				Y	Y				Y	Y	Y	Y			Y	Y

* = Plus all other TSP intersections.

Table 2-1 (Continued)

Destructive Workscope

Defect Evaluation	68-46					72-49				
	1	2	3	14	18	2	5	7	13	17
	LTS	LTS	LTSF-1st Span	7th TSP	9th TSP	LTSF	2nd TSP	3rd TSP	7th TSP	9th TSP
	Y.Dep	Y.Dep	IGA	WEAR	WEAR	IGA	NDD	NDD	WEAR	WEAR
- Visual/Stereovisual Insp.	Y	Y	Y	Y	Y	Y	Y	Y	Y	Y
- Section		Y		Y		Y	Y	Y		Y
- SEM		Y				Y				Y
- Replica				Y	Y				Y	
- De-scale				Y	Y	Y			Y	Y
- Visual/Stereovisual Insp.				Y	Y	Y			Y	Y
- Dimensions of Defects				Y	Y				Y	
- Tube Swelling			Y							
- Burst Testing	Y		Y	Y	Y	Y	Y	Y	Y	
- Visual/Stereovisual Insp.			Y	Y	Y	Y	Y	Y	Y	
- SEM of Deposit Flake			Y							
- SEM/EDS/WDS			Y	Y	Y				Y	Y
- Defect Metallography			Y			Y				Y
- SEM of Met Sample										
- SAM/XPS			Y							
- XRD (Thin Film)			Y							

Defect Evaluation	109-71		136-26			41-44	72-49	109-71	68-46	109-71
	7	14	2	9	15	2	3	13	15	15
	3rd TSP	7th TSP	LTSF	3rd TSP	7th TSP	LTSF	Rust Nodule	Rust Nodule	White Streak	White Streak
	WEAR	WEAR	NDD	NDD	WEAR	IGA				
- Visual/Stereovisual Insp.	Y	Y	Y	Y	Y	Y	Y	Y	Y	Y
- Section	Y	Y			Y					
- SEM	Y	Y			Y					
- Replica	Y									
- De-scale	Y*			Y	Y					
- Visual/Stereovisual Insp.	Y			Y	Y					
- Dimensions of Defects	Y	Y								
- Tube Swelling			Y	Y						
- Burst Testing						Y				
- Visual/Stereovisual Insp.			Y	Y		Y				
- SEM of Deposit Flake			Y							
- SEM/EDS/WDS	Y				Y	Y	Y	Y	Y	Y
- Defect Metallography	Y	Y			Y	Y	Y	Y	Y	Y
- SEM of Met Sample							Y	Y	Y	Y
- SAM/XPS						Y				
- XRD (Thin Film)						Y				

Y.Dep = Spots of Yellow Deposit   Y* = Metallography was done prior to de-scale

Table 2-1 (Continued)
Destructive Workscope

Deposit Analyses	68-46					136-26				
	3	6	10	13	17	4	8	11	14	18
	1st Span	3rd Span	5th Span	7th Span	9th Span	1st Span	3rd Span	5th Span	7th Span	9th Span
- Swell & Collect Deposit	Y	Y	Y	Y	Y	Y	Y	Y	Y	Y
- Elemental Anal. (ES/ICP/FAA)		Y	Y	Y	Y	Y	Y	Y	Y	Y
- Total Carbon (Perkin Elmer)		Y	Y	Y	Y	Y	Y	Y	Y	
- Total Sulfur (ICP or Turb.)		Y	Y	Y	Y	Y	Y	Y	Y	
- XRD (Bulk)		Y	Y	Y	Y	Y	Y	Y	Y	Y
- SEM/EDS/WDS (Flakes)	Y	Y	Y	Y	Y	Y	Y	Y	Y	Y
- Metallography (Flakes)		Y	Y	Y	Y	Y	Y	Y	Y	Y
- SEM/EDS/WDS (Metallography Flakes)		Y	Y	Y	Y	Y	Y	Y	Y	Y
- Loading (Met. & Cleaning)	Tube Sections 136-26-3, 7, 14, 17, & 21									
- Density & Porosity	Samples from 136-26-8, 11, 13, & 14									
- Isotopic Analyses	Tube Sections 136-26-3 & 21									

Base Metal Characterization	68-46	72-49	109-71	136-26	41-44
	21&8	20&14	20&8	21&7	5&3
- Tensile Testing	Y	Y	Y	Y	Y
- Burst Testing	Y	Y	Y	Y	Y
- Metallography (Dual Etch)	Y	Y	Y	Y	Y
- Microhardness Testing	Y	Y	Y	Y	Y
- Bulk Chemistry	Y	Y	Y	Y	Y
- Sensitization Testing (Huey)	Y	Y	Y	Y	Y

Table 2-2: Burst Pressure Test Results

TUBE NUMBER	DEFECT LOCATION	BURST PRESSURE (psi)	COMMENTS
68-46	LTS/1st Span	7000[1]	Burst at IGA defect that leaked during swelling
	7th TSP	10850	Burst initiated at wear mark
	9th TSP	10700	Burst initiated at wear mark
	defect-free	10850	Burst in freespan
72-49	LTS/1st Span	10650	Burst initiated at small IGA patch
	2nd TSP	10650	Burst in freespan just above TSP region
	3rd TSP	10650	Burst outside TSP region
	7th TSP	10550	Rupture passes through wear mark, but did not initiate at it
	10th TSP (defect-free)	10550	Burst outside TSP region
109-71	defect-free	11100	Burst in freespan
136-26	defect-free	10750	Burst in freespan
41-44[2]	LTS/1st Span	9800	Burst initiated at small IGA patch
	defect-free	10100	Burst in freespan
97-91[2]	defect-free	10450	Burst in freespan
106-32[2]	defect-free	11250	Burst in freespan

NOTES:
1. The burst pressure reported in the table for tube number 68-46-3A has been adjusted for the presence of the brass shim.
2. Tube pulled in 1992.

Table 2-3: Field NDE Results vs Destructive Examination Results

Tube Number (Row/Column)	Location inches	Defect Identification	Field Bobbin Call	Defect Dimensions, 10^{-3} inches			
			Volts (%TW)	Maximum Depth (%TW)	Axial Length	Width	Volume (in^3)
68-46	LTSF - 0.60	pit-like IGA	NDD	28.0 (75%)	228	89	$138(10)^{-6}$
	7th TSP - 0.56	"D"-shaped wear	1.36(27%)	12.0 (32%)	90	119	$68(10)^{-6}$
	9th TSP + 0.81	Tapered wear	0.65(S/N)	7.0 (19%)	425	141	$157(10)^{-6}$
	9th TSP - 0.58	Tapered wear	0.38(S/N)	4.9 (13%)	515	148	$135(10)^{-6}$
72-49	Below LTSF	pit-like IGA	NDD	7.0 (19%)	41	29	$2(10)^{-6}$
	7th TSP - 0.69	Oval wear	0.50(39%)	6.0 (16%)	94	134	$35(10)^{-6}$
	9th TSP + 0.82	Tapered wear	0.49(S/N)	3.8 (10%)	640	134	$62(10)^{-6}$
	9th TSP -	Tapered wear	NDD	[redacted]	812	145	[redacted]
109-71	3rd TSP - 0.67	"D"-shaped wear	0.17 (S/N)	5.0 (14%)	86	97	$17(10)^{-6}$
	7th TSP - 0.68	Circular wear	0.17(40%)	12.2 (33%)	112	101	$66(10)^{-6}$
136-26	LTSF	None	LC1 @ LTS	[redacted]			
	3rd TSP	None	NDD	[redacted]			
	7th TSP - 0.70	"D"-shaped wear	1.29(31%)	13.0 (35%)	112	170	$68(10)^{-6}$

Table 2-4: Materials Properties Summary

PROPERTY		TUBE IDENTIFICATION				
		68-46	72-49	109-71	136-26	41-44
Yield Strength, ksi		49.5	46.4	49.5	45.9	42.3
Ultimate Tensile Strength, ksi		102.6	100.2	102.5	102.9	96.5
Reduction in Area, %		24.9	24.1	24.9	26.8	22.4
Burst Strength, psi		10,850	10,550	11,100	10,750	10,100
Microhardness	ID	186.7	189.2	194.2	188.2	176.9
HV	Midwall	175.8	170.2	181.6	188.5	168.1
	OD	184.3	187.8	198.3	182.3	177.8
Grain Size		7.8	7.6	8.0	6.7	6.4
Carbide Distribution		*	*	*	*	*
Sensitization Test (Modified Huey), mg/dm^2/day		3289 **	6012 **	992	1199	2028 **
Composition, %	C	0.047	0.034	0.041	0.033	0.035
	S	<0.001	0.003	<0.001	0.003	0.002
	P	0.014	0.012	0.008	0.008	0.013
	Fe	7.11	7.37	6.94	7.26	6.90
	Cr	14.09	15.29	15.15	15.06	14.66
	Mn	0.29	0.31	0.32	0.30	0.31
	Co	<0.05	0.052	0.050	<0.05	<0.05
	Cu	<0.05	<0.05	0.054	<0.05	<0.05
	Si	0.37	0.28	0.33	0.28	0.34
	Al	0.067	0.11	0.21	0.11	0.12
	Ti	0.13	0.18	0.21	0.16	0.21

* - Carbides are predominately intergranular, with apparent decoration on the grain boundaries.

** - Huey test samples disintegrated prior to completion of the full 48 hours of testing

Section 3

DISCUSSION OF RESULTS

3.1 Observed Tubewall Degradation

Tube degradation that occurred in the Crystal River-3 "B" steam generator, as evidenced by the sections of removed tubing, can be placed into two categories:

1. Intergranular degradation that occurred in the lower tubesheet crevice and first tube span, and

2. Mechanical wear at the contact points between the tube and tube support plate lands.

No other forms of degradation were found in either this examination or in the examination of archived tube sections removed in 1992. No degradation was found at locations where distorted tubesheet signals were observed in the field by EC testing. Conclusions regarding these two types of defects are discussed below.

3.1.1 *Intergranular Degradation*

The intergranular degradation found within the lower tubesheet crevice region of tubes 68-46 and 72-49 was located within the first 2 inches below the LTSF for tube 68-46; and within the first 5 inches below the LTSF for tube 72-49. Four (4) spots of IGA were found in the free span of tube number 72-49. Metallography confirmed the degradation on 68-46 at which burst occurred to be intergranular in nature and EDS/WDS detected a sulfur-rich corrosion film on the grain facets. Results from the Scanning Auger Microscopy/X-Ray Photoelectron Spectroscopy (SAM/XPS) analysis of the corrosion film indicate that the IGA fracture surface is covered with a duplex film (Reference 6). The outer layer is nickel oxide. After one micron of sputtering, sulfur is found, probably as nickel sulfide.

In the previous examination of tubes removed from Crystal River-3, similar spots of IGA were seen to occur in a region extending from ~6 inches below to 18 inches above the secondary face of the lower tubesheet. It was concluded in Reference 3 that the observed corrosion was likely caused by reduced sulfur species while at low temperatures (<170°F) sometime during the period from startup in 1977 to early 1980. The source of sulfur was postulated to be either chronic leakage of cation resin from the condensate polishers or a significant intrusion of sulfur contaminant. It was further postulated that propagation (of the IGA) ceased when conditions were no longer favorable to corrosion. A review of prior eddy current data for the 1992 pulled tubes was consistent with this hypothesis, suggesting that the IGA initiated as early as 1980 and is currently dormant or at least growing very slowly.

For the present case, it is postulated that the corrosion mechanism is the same as postulated in Reference 3; i.e., reduced sulfur IGA. This conclusion is based on the following observations:

1. The defects are intergranular in nature and confined to the same regions of the tube as reported in Reference 3; i.e., 6 inches below to 18 inches above the lower tubesheet secondary face. Inasmuch as the tubes are not expanded into the tubesheet, a path for contaminant ingress into the crevice exists.

2. Sulfur is present within the corrosion film present on the grain facets, probably as nickel sulfide. It has been well established that TSG tubing is susceptible to intergranular attack in acidic solutions containing reduced sulfur oxyanions (Reference 4). Further, sensitized Alloy 600 tubing is far less susceptible to intergranular stress corrosion cracking in caustic environments than is mill annealed Alloy 600 (Reference 5). Additional evidence that caustic-forming species are not involved in the tubesheet crevice region corrosion is the limited depth within the tubesheet crevice that IGA was found. Experience with unexpanded tubesheet crevices in recirculating steam generators (RSGs) has shown that a concentrated caustic solution can exist throughout the whole crevice region and lead to intergranular corrosion deep within the crevice. Further, the OTSG lower tubesheet is subjected to primary system cold leg temperatures, whereas, most caustic-induced IGA has occurred in RSG hot legs.

3. Corrosion film data from the analysis being performed at Rockwell International (Reference 6) indicates the presence of a duplex corrosion film on IGA grain facets, with sulfur incorporated in the inner film. This suggests that the environment responsible for the initial attack may no longer be present; i.e., the reduced sulfur species have been depleted and the corrosion process has stopped.

The elemental sulfur deposits observed in the first tube span and within the lower tubesheet crevices may or may not be associated with the intergranular defects. Elemental sulfur is not in the right oxidation state to initiate IGA; although changing environmental conditions during startup, shutdown, and layup could create conditions which could make the sulfur aggressive. Since there is not a direct correlation of the IGA patches with the spots of yellow deposit, it is concluded that the yellow sulfur deposits do not pose a significant corrosion risk.

3.1.2 *Tube-to-TSP Wear Defects*

There were two types of defects observed at the tube-to-TSP land contacts: at the 7th TSP and 3rd TSP, oval or "D" shaped wear marks were found at the lower edge of a tube support land; at the 9th TSP, tapered wear marks were found at both the upper and lower edges of the support plates. Tapered wear has been observed in tubes pulled previously from other OTSGs (Reference 7). The oval or "D" shaped wear was not observed in previously pulled OTSG tubes, but has been observed in recirculating steam generators as described in Appendix B.

No conclusive evidence of corrosion was found in the wear marks. Therefore, it is concluded that the degradation was the result of mechanical wear from the tube rubbing against the tube support plate land, or against oxides or other debris wedged between the tube and TSP land (abrasive wear). Appendix B includes a description of wear observed in nuclear steam generators and a discussion of industry experience with the detection of wear.

Based on the observation that these defects were present as early as 1985 at the 7th TSP for tube 136-26, it is concluded that their rate of growth is minimal, and that this mode of degradation is both easily monitored and managed. Previous review of 607 wear indications (Reference 8) also concluded that wear growth is slow in OTSGs. As demonstrated, the effect of the wear defects on burst pressure is minimal.

An additional growth rate study of selected S/N indications from both OTSGs at Crystal River-3 was performed utilizing Refuel 9 data (Reference 15). This study determined growth rate for indications present in the freespan and tubesheet regions for each steam generator in order to determine if growth rates differed by location and/or by steam generator. Results of Reference 15 confirm previous conclusions of essentially no growth of S/N indications, at either location, within the CR-3 OTSGs.

3.2 Structural Integrity Implications

3.2.1 *Pit-like IGA*

In a previous submittal to the NRC (see Reference 1), the structural margins specified in Regulatory Guide 1.121 were shown to be met for 100% through wall axial cracks equal to or less than 0.25 inch in length; 100% through wall circumferential cracks equal to or less than 122° in total circumferential extent were also shown to meet the required structural margins. An axial limit of 0.33 inches was proposed in a subsequent submittal (Reference 14), but the discussion herein continues to perform assessment against the 0.25 inch value, since this is reflective of the largest indication found within the pulled tubes. A total of nine burst tests (see Tables 3-1 and 3-2) are now available on pulled tubes from Crystal River-3. These burst tests indicate that expected structural margins are conservative as discussed below.

Table 3-1 lists burst tests results on undegraded sections of five pulled tubes from Crystal River-3. This burst test data establishes baseline, undegraded burst pressures. Calculated undegraded burst pressures from yield and ultimate strength values agree well with actual measurements.

Burst pressures of 1992 and 1994 pulled tube sections with pit-like IGA are listed in Table 3-2. The burst modes of these tube sections were axial. Hence these burst test results reflect the ability of tubes with IGA degradation to meet the required burst strength margin of 3 times the normal operation pressure differential, i.e. 4050 psi. The lowest measured burst pressure is 7000 psi for tube section 68-46-3 with a IGA patch 0.6 inch below the LTSF. By comparison, for a tube with lower bound tensile properties (95% probability, 95% confidence), the corresponding burst pressure would be 5848 psi. This conservative value is also well above the required value of 4050 psi.

As illustrated in Table 3-2, there are a number of approaches which may be followed in calculating the burst pressure of tubes with local regions of IGA. One extreme bounding model would be to assume uniform thinning around the circumference of the tube and apply the burst equation of NUREG/CR-0718 (Reference 9). The axial burst mode suggests the use of partial through wall axial crack models. Several have been applied. These include the Framatome equation (Reference 10) and two similar models (References 11, 12) where the burst pressure is a linear function of depth of degradation between the undegraded burst pressure and that of a through wall crack. These are designated the PNL Slot equation and the Begley-Houtman-Keating, BHK, equation.

Figure 3-1 illustrates a comparison of burst pressure predictions from these equations for a degradation length of 0.25 inches. The degradation depth is expressed as a fraction of the tube wall thickness. For conservatism, lower 95/95 tensile properties are assumed. At shallow degradation depths, burst pressure predictions are very similar. At large depths of degradation, the uniform thinning model must extrapolate to zero burst pressure at through wall penetration. The partial through wall axial crack models extrapolate to the through wall crack burst pressure limit.

The best experimental burst pressure determination for through wall axial cracks in steam generator tubes has been performed by Hernalsteen (Reference 13). Very high flow capacity tests eliminated the need for sealing bladders of any description and settled the question of the effect of sealing systems on burst pressure measurements. The BHK model extrapolates to a through wall limit below the Hernalsteen value as does the PNL Slot equation and hence are conservative in the limit of a through wall crack. Figure 3-1 demonstrates that there is margin beyond the $3\Delta P$ requirement for a 0.25 inch long, 100% through wall crack.

The burst pressure for tube section 68-46-3 with a 0.25 inch long region of degradation (the actual degradation length is 0.228 inch, but was rounded up to 0.25 inch for this

discussion) is also plotted on Figure 3-1. For conservatism, the measured burst pressure was reduced to match the assumption of lower limit tensile properties. When burst strength is computed on the basis of the maximum depth of degradation (a value of 70% was assumed), the measured burst pressure lies above predictions from all models, but is closest to the BHK model. The same statement is true for all of the test results in Table 3-2. Pulled tube burst test results are consistent with expectations of structural evaluations and behave in a consistent, predictable fashion.

The degradation present in tube 68-46 is consistent with the range of morphologies observed to date at Crystal River-3 which have been dispositioned with a combination bobbin voltage and RPC sizing criteria. The mode of degradation is considered to be static as supported by evaluation of past NDE records. The degradation evident in tube 68-46 just below the top of the LTS was not detected during field inspection. This is consistent with other industry experience with this damage mechanism. There is a chance that degradation on the order of that experienced by tube 68-46 may not be detected by NDE in other tubes. The demonstrated margin of tube 68-46 with respect to structural requirements and the static nature of the degradation show that this possible circumstance does not pose a threat to structural margins.

3.2.2 *Wear*

Table 3-3 shows the burst testing results from four tube sections containing wear degradation. The burst pressures of the degraded tube sections are compared to the burst pressures for undegraded sections of the same tubes using data from Table 3-1. As can be seen from Table 3-3, the wear scars had practically no detrimental effect on the tube burst pressure. The wear observed on the pulled tubes is therefore concluded to also pose no threat to the structural margins.

3.3 Leakage Integrity Implications

Helium leak testing was performed on eight (8) sections of the 1994 pulled tubes and the 1992 archived tube that contained eddy current indications as shown in Table 2-1. No leaks were found in the 8 sections that were tested. In a previous submittal (Reference 1), it was shown that the minimum tube wall thickness required to avoid developing a leak during a main steam line break (MSLB) accident was 8% of the tube wall. A defect with a depth of 92% through wall would thus not leak at a tube differential pressure of 2250 psi imposed during a MSLB. The minimum wall thickness for a higher tube loading of 2600 psi was also calculated in Reference 1. The maximum defect depth that would not leak at 2600 psi was calculated to be 87% through wall. The deepest defect in the 1994 pulled tubes was ~75% through wall. Therefore, previous leakage considerations concerning the pit-like IGA are presently still valid, and the 1994 S/N plugging criteria has been effective in not leaving potential leaking tubes in service.

3.4 NDE Field Detection Capabilities

In comparing the 1992 and 1994 EC field data for the four 1994 pulled tubes, it was found that the probability of detection (POD) for the intergranular degradation was consistent with that reported in Reference 1 for the 1992 pulled tubes.

NDE detection and sizing performance on the Crystal River-3 pulled tubes is a BWOG SG Committee project. Bobbin 0.510" MF and HF, and 0.540" MF and HF probes; 0.080" and 0.115" RPC probes; RFEC; and UT were all utilized in the field inspection of the pulled tubes. This data will be integrated into the BWOG Tube Integrity Project to provide POD and sizing accuracy of the various NDE techniques for different defects: field, laboratory grown, and machined.

The next phase of this BWOG task will compare all of the field NDE for pulled tubes to the metallurgical results to determine the POD and sizing accuracy (% through wall, length, width) for each probe type/technique utilized in the field inspections. Scatter plots for IGA and wear will be utilized to show length and width as called in the field vs. laboratory metallurgical results, and % through wall where appropriate, for each inspection technique used. The Oconee Unit 1 pulled tubes will be included in this task at a later date. This BWOG task will be performed in 1995.

Table 3-1. Undegraded Burst Pressure

TUBE	YIELD STRENGTH (psi)	ULTIMATE STRENGTH (psi)	MEASURED BURST PRESSURE (psi)	CALCULATED BURST PRESSURE (psi)
68-46	49500	102600	10,850	10500
72-49	46400	100200	10,550	10120
109-71	49500	102500	11,100	10493
136-26	45900	102900	10,750	10272
41-44*	42300	96500	10,100	9582
97-91*	46800	97500	10,450	9961
106-32*	46000	100900	11,250	10141

* Tube pulled in 1992.

Table 3-2. Burst Pressure of Tubes with IGA Degradation

TUBE SECTION	DEGRADATION LENGTH (inches)	MAXIMUM DEGRADATION DEPTH (% TW)	MEASURED BURST PRESSURE (psi)	CALCULATED BURST PRESSURE (psi) (FRAMATOME EQUATION)	CALCULATED BURST PRESSURE (psi) (BHK EQUATION)	CALCULATED BURST PRESSURE (psi) (UNIFORM THINNESS EQUATION)	CALCULATED BURST PRESSURE (psi) (PNL SLOT EQUATION)
41-44-2[1]	0.069	54	9800	7155	8746	8705	8410
72-49-2	0.041	19	10650	9638	9945	9998	9848
68-46-3	0.228	75	7000	4548	6705	5654	5996
97-91-2[1]	0.076	54	10300[2]	7305	9022	8968	8636
106-32-2[1]	0.062	40	10900[2]	8417	9568	9643	9305

NOTES:
1. Tube pulled in 1992.
2. 1992 burst pressure adjusted per discussion in Appendix A.

Table 3-3. Burst Pressure of Tubes with Wear Degradation

TUBE SECTION	MAXIMUM DEGRADATION DEPTH (%TW)	MEASURED BURST PRESSURE (PSI)	% OF UNDEGRADED BURST PRESSURE
68-46-(7th TSP)	32%	10,850	100%
68-46-(9th TSP)	19%	10,700	99%
72-49-(3rd TSP)	No Wall Loss Observed	10,650	101%
72-49-(7th TSP)	16%	10,550	100%

NOTE: Maximum degradation depth reported is as determined by destructive examination. Undegraded burst pressure for tubes are shown in Table 3-1.

CALCULATED BURST PRESSURE VERSUS RELATIVE DEGRADATION DEPTH FOR A CRACK LENGTH OF 0.25 INCH

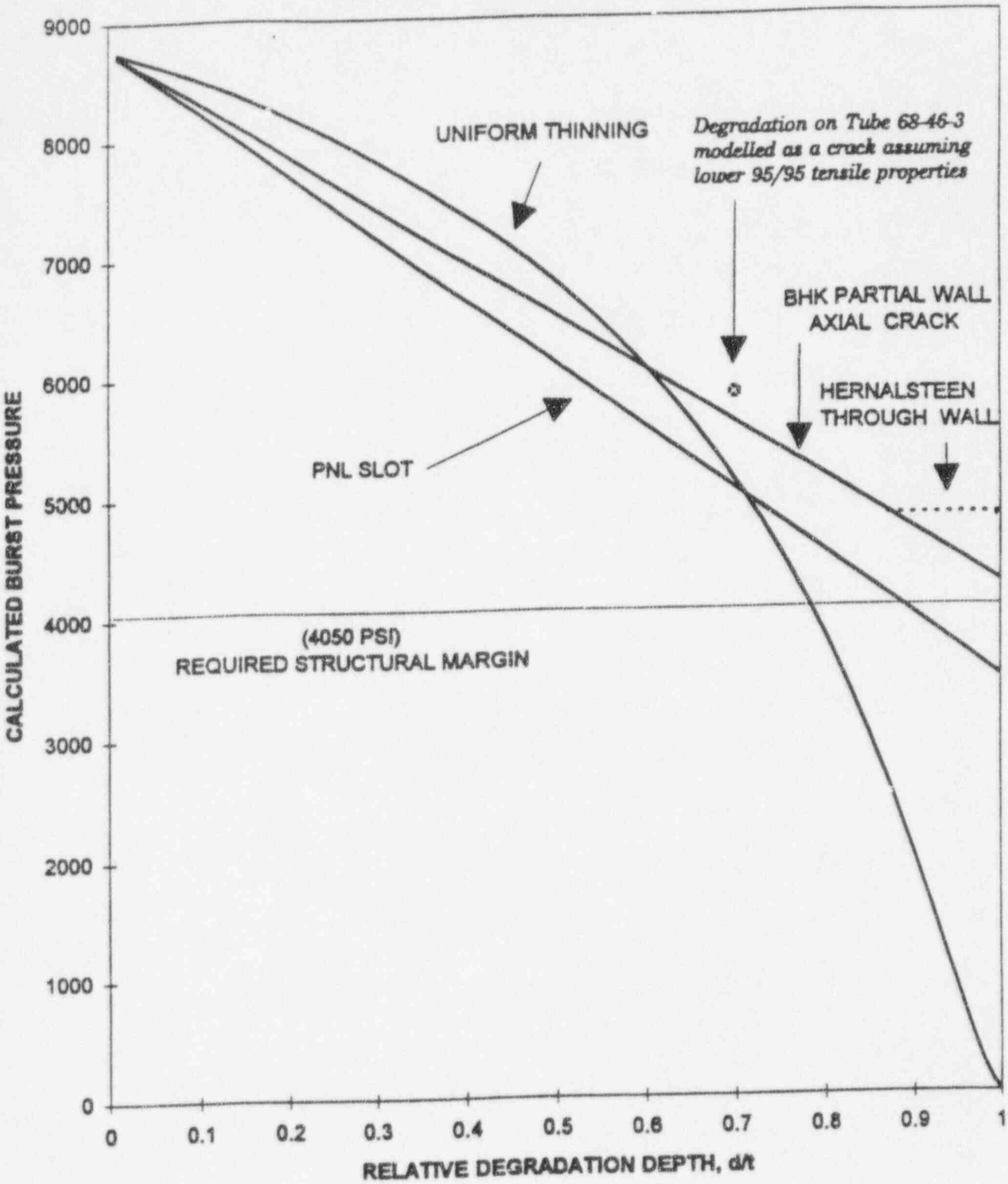

Figure 3-1

Section 4

CONCLUSIONS

Based on results from the nondestructive and destructive examination of sections of tubing removed from the Crystal River-3 steam generators during the Refuel 9 outage, the following conclusions have been reached:

1. Two types of tube damage mechanisms are present in the Crystal River-3 "B" steam generator:

   - Intergranular degradation in the lowermost tube span and within the tubesheet crevices near the lower tubesheet secondary face.

   - Mechanical wear at the contacts between the tube and tube support plate lands.

2. The intergranular degradation was caused by reduced sulfur species that resulted from an intrusion of sulfur contaminant or from chronic leakage of cation resin from the condensate polishers in the late 1970's or early 1980's. The degradation is similar to the pit-like IGA found in tubes removed from Crystal River-3 during Refuel 8 (1992), and is no longer active. As demonstrated by burst tests, these defects do not pose a threat to structural margins.

3. The growth rate of wear defects observed at tube support plates is slow and easily monitored. As demonstrated by tests performed in the laboratory, the effect of these wear scars on burst pressure is minimal. As such, they do not pose a threat to the structural integrity of the tubing.

Section 5

REFERENCES

1. Florida Power Corporation letter to NRC, 3F0494-09 dated April 19, 1994.

2. Robert F. Keating, Memo to D. Steininger (EPRI) dated October 25, 1993, "EPRI Guidelines for Leak & Burst Testing of SG Tubes," NSD-EPRI-0545.

3. EPRI TR-103756, "Examination of Crystal River Unit 3 Steam Generator Tube Sections," Final Report, April 1994.

4. EPRI NP-4504-LD, "Evaluation of Alloy 600 Tube A77-34 from Steam Generator A of Arkansas Nuclear One, Unit 1," March 1986.

5. D.W. Koch and B.P. Miglin, "Literature Review - OTSG Secondary-Side Tube IGA/SCC Evaluation," B&W Nuclear Technologies, Report No. 51-1177882-00, January 1990.

6. Draft Final EPRI Report titled "Failure Analysis of Steam Generator Tubing from Crystal River Unit 3," EPRI Research Project S413-12, dated December 1994.

7. "OTSG Pulled Tube Catalog", B&W Report 1190991, December 1988.

8. K.S. Hagedon, "Crystal River 3 OD Wear Growth," B&W Nuclear Technologies, Report No. 51-1203897-00, July 1991.

9. Alzheimer, J.M., Clark, R.A., Morris, C.J., Vagins, M., "Steam Generator Tube Integrity Program Phase I Report", NUREG/CR-0718, Sept., 1979.

10. Framatome

11. Kurtz, R.J., Bickford, R.L., Clark, R.A., Morris, C.J., Simonen, F.A. Wheeler, K.R., "Steam Generator Tube Integrity Program", Phase II Final Report, NUREG/CR-2336, August, 1989.

12. Begley, J.A., Keating, R.K. and Houtman, J.L., to be published.

13. Hernalsteen, P., "The Influence of Testing Conditions on Burst Pressure Assessment for Inconel Tubing," International Journal of Pressure Vessels and Piping, Vol. 52, 1992, pp. 41-57.

14. Letter from FPC to NRC, "Technical Specification Change Request No. 203", dated May 31, 1995.

15. S. D. Brown, "Crystal River 3 8R/9R Bobbin Voltage (S/N) Growth Rate Calculations" Packer Engineering Report B51956-R1, dated May 1995.

APPENDIX A

ESTIMATE OF BURST PRFSSURES FOR CRYSTAL RIVER 3 STEAM GENERATOR TUBING BURST TESTED IN 1992

APPENDIX A

ESTIMATE OF BURST PRESSURES FOR CRYSTAL RIVER 3 STEAM GENERATOR TUBING BURST TESTED IN 1992

Background

Two sections of tubing from Crystal River 3 (CR-3), 97-91-2 and 106-32-2, were burst tested during a steam generator tube examination in 1992 (Reference 1). The burst pressures obtained in that testing were high compared to testing done recently in the 1994 CR-3 steam generator tube examination. Specifically, sample 97-91-2, which contained several small patches of pit-like IGA, had a 1992 burst pressure of 12,400 psi, which is 1,950 psi higher than the 10,450 psi burst pressure determined in 1994 for the defect-free section 97-91-5. Similarly, the burst pressure of sample 106-32-2, which also contained several small patches of IGA, was reported to be 11,400 psi, which is 150 psi higher than the 11,250 psi burst pressure determined in 1994 for the defect free section 106-32-5.

This report discusses these differences, and provides best estimates to adjust the 1992 data to be consistent with current burst testing procedures.

Differences in Test Methods

The 1992 testing differed from the 1994 testing in several ways. The 1992 testing was consistent with past practices, which had been adapted from procedures developed for the burst testing of Zircalloy fuel cladding tubes. The data obtained in 1992 were consistent with and comparable to past burst test data from other steam generator tubes. Sample pressurization rates were rapid, with the intent being to pressurize the sample to failure in less than 10 seconds (the actual goal was failure in about 5 seconds). Testing in 1994, in contrast, pressurized the tubes at a rate of 1000 to 2000 psi/second in the elastic region of the test (i.e., prior to the yield pressure of the tube), per recently-developed EPRI guidelines for burst testing. At these rates, the total time to failure is about 60 seconds.

Proposed Source of Error

One difference in the test methods used is the volume flow rate required to achieve the desired pressurization rates. High volume flow rates are believed to give rise to a significant friction head loss in the system, adding a back-pressure error at the pressure sensing point.

In 1992, the rapid pressurization rates used required hydraulic volume delivery rates such that flow velocities in the 0.062" inner diameter high pressure tubing averaged about 14 feet/second. In contrast, pressurization rates in 1994 translated to flow

velocities of only about 0.4 feet/second. The high fluid velocities in the 1992 testing are believed to be capable of giving rise to frictional head loss errors. This is illustrated in Figure 1.

To demonstrate the existence of such a friction loss error, de-ionized water was vented to atmosphere at high flow rates using the 1994 burst test apparatus. The water was vented from the accumulator through the tubing normally used in testing and through the fitting where a S/G tube sample would normally be. Although the "sample pressure" was zero by definition, pressures of several thousand psi were recorded by the pressure transducer. The 1994 burst test apparatus is instrumented to allow the delivered volume to be monitored and recorded, and from this, the pressure as a function of volume flow rate could be graphed and modelled, (see Figure 2). It can be seen that virtually no error is expected at the low volume rates used in the 1994 testing, but that errors can be expected at volume rates above about 1 cubic inch per second.

Using this model of the flow error versus volume delivery rate, the data of tests on virgin steam generator tubing carried out at high pressurization rate were corrected to remove the error; this is shown in Figure 3. The instantaneous volume delivery rate during each test was calculated, converted via the model to a flow rate error, and the error subtracted from the recorded pressure to yield corrected pressures. The results validate the concept of the flow rate error.

Correction of the 1992 Data

Since the 1994 data were obtained in accordance with the EPRI guidelines (Reference 2), for which the error due to flow rate is negligible, no correction is required. The 1992 burst pressure data, however, must be corrected to account for the aforementioned high flow rate.

Three independent approaches can be used to estimate the burst pressures of sections 97-9-2 and 106-32-2 that would have been measured had the current burst test procedure been used:

1) Estimating and subtracting the error caused by the high flow rates used in 1992 test procedure,

2) Estimating the burst pressures using empirical equations relating defect geometry to burst pressure (combined with the 1994 burst pressures of defect free tubing), or

3) Estimating the burst pressures using the actual uniform diametrical strain achieved in the 1992 testing (measured on archived tube sections) and a pressure versus diametrical strain curve obtained from the 1994 testing of

defect free tubing. These curves are only recently available due to new instrumentation added to the burst test apparatus. This method is expected to be the most accurate.

Method 1 - Subtraction of the Flow Rate Error

In 1992, the burst pressure for tube 106-32-2 was reported to be 11,400 psi; this was the pressure as determined by a follower on a Heise pressure gage in the system. The pressure recorded by a pressure transducer (which a calibration check showed to be accurate) was 11,100 psi. Based on experience gained with the follower since 1992, we believe that at the high pressurization rate used, the follower's momentum caused it to overshoot the actual maximum pressure of the test. We now believe that the transducer's maximum of 11,100 psi is the maximum pressure (without correction) of this test.

The testing of sample 106-32-2 was carried out using the same burst test apparatus as was used in 1994; the error model presented above can be applied to this 1992 data. (Although several slight modifications were made to the apparatus between 1992 and 1994, these are not considered significant to the current problem.) Volume flow rate data are not available for the 1992 test, but these can be assumed for each point in time during the test.[1]

The data and calculations for this correction are listed in Table 1.[2] The volume flow rates used in this test were not so great that a large error was introduced by the flow. Only a 56 psi error was occurring at the end of the test (at burst), and the corrected burst pressure (11,040 psi) is only slightly different than the originally recorded pressure (11,100 psi). This is 150 psi lower than the burst pressure of section 106-32-5 (defect free) done in 1994, and is in good agreement with the burst pressure estimated by Method 3 below.

---

[1] Three constraints govern the choices of assumed volume flow rates. First, the integral of the flow rate should equal the total displacement volume required to strain the sample to burst. Second, the shape of a pressure versus integral volume curve constructed from the assumptions should resemble those of other CR-3 steam generator tubing. Third, the volume flow rates should vary throughout the test per an expected pattern; that is, should be monotonically increasing with time (as the operator continuously opened the throttle valve during test), but perhaps with step wise increases (as the operator opened the valve more rapidly in response to the pressurization rate slowing down after yield and at other points in the test).

[2] The data in Table 1 meet the constraints listed above. The assumed volume flow rates in Table 1 follow the expected pattern: rates are low during the elastic portion of the curve, increase step-wise after yield is detected, and increase smoothly thereafter. The integral volume at burst (2.42 cu.in.) is in agreement with the volume expected to be required to strain this 30.7 inch sample to its final strain of 12.9% (2.23 cu.in). Finally, the corrected pressure versus integral volume has a shape similar to those obtained from other Crystal River 3 tubes.

In the case of sample 97-91-2, it is not possible to apply this correction model to the data. The general concept that the 1992 data is high by about 2000 psi because of a flow head loss error still appears to be valid, but a straight forward correction is not possible. The testing of sample 97-91-2 in 1992 was done using a different apparatus, which used hydraulic oil rather than water as its working fluid. The flow rate error behavior of this apparatus using the more viscous oil is unknown. It is possible to assume a flow rate error model that will correct the pressures down to those comparable to the data obtained on sample 97-91-5 in 1994, but minor changes in the error model parameters and/or the assumed flow rates produce large changes (100's of psi) in the corrected pressure.

Method 2 - Empirical Models of the Effect of Defects on Burst Pressure

Prior work has been done to determine and model the effect of defects on the burst pressure of steam generator tubing (Reference 3). This work has concentrated primarily on cracks and large wastage areas. A brief literature search did not reveal any testing or modeling on small (1/16" diameter) IGA patches, pits, or drilled holes. Nevertheless, the results of modeling on uniform thinning can be used to indicate a lower bound of the burst pressure that can be expected given the presence of defects of the dimensions discovered in the 1992 testing.

Table 2 presents the results of these models, applied to the tubes 97-91-2 and 106-32-2. As a calibration check, this model was also applied to tube 41-44-2, which had similar IGA patches and for which valid 1994 burst data exist. The model for uniform thinning provides reasonable numbers, but does reduce the burst pressure of 41-44-2 excessively compared to the experimental data. Nevertheless, the predictions for tubes 97-91-2 and 106-32-2 can be used as lower bounds of the burst pressures.

Method 3 - Estimates based on Diametrical Strain

Figure 4 shows the 1994 burst test data for tube sections 41-44-5 (defect free) and 41-44-2 (IGA patches), both converted to pressure versus diametrical strain. To convert to diametrical strain, the delivered hydraulic volume data recorded during testing (only recently made available by new instrumentation added to the test apparatus) were scaled and offset such that the resulting value at burst agreed with the diametrical strain determined from post test diameter measurements. It can be seen that the small IGA patches had virtually no effect on pressure versus strain behavior up to the point of burst. This behavior is consistent with the behavior of load versus strain data for the tensile testing of notched ductile materials.

Figures 5 and 6 show the 1994 burst test data for tube sections 97-91-5 and 106-32-5 (both defect free), similarly converted to pressure versus diametrical strain curves. (Both of these curves have been corrected for volume lost to a fitting leak that occurred during the tests. The curve for section 106-32-5 is a composite of three

attempts to swell and burst this section.) The arrows on these graphs indicate the diametrical strain at burst determined from post test diameter measurements of sections 91-91-2 and 106-32-2. The pressures at these strains are best estimates of the burst pressures of the 1992 tests. These pressures are 10,300 psi for tube 97-91-2 and 10,915 psi for tube 106-32-2.

Conclusions

The differences between burst pressures obtained in 1992 and 1994 were caused by a friction head loss error resulting from the high flow rates necessary to achieve the high pressurization rates used in the 1992 testing. With regard to recently adopted burst test procedures per EPRI guidelines, the 1994 data are considered valid, and the 1992 data require adjustment.

The hypothetical burst pressure for the sections 97-91-2 and 106-32-2 tested per the 1994 test procedures were estimated by three independent methods. Table 3 summarizes the burst pressure values for the three methods. Because of the excellent fit to experimental data shown by the method 3 (estimating based on diametrical strain), it is concluded that method 3 provides the best estimate of the burst pressure for the samples tested in 1992.

References

1. EPRI TR-103756, "Examination of Crystal River Unit 3 Steam Generator Tube Sections," Final Report, April 1994.

2. Memo, Robert Keating (Westinghouse) to D. Steininger (EPRI) dated October 25, 1993, "EPRI Guidelines for Leak & Burst Testing of SG Tubes," NSD-EPRI-0545.

3. D. Azodi, H. Schulz, and R. Arenz, "On the Integrity of Steam Generator Tubes and Plugging Assessment", Transactions of the 9th International Conference on Structural Mechanics in Reactor Technology, August 17-21, 1987, Vol. D, page 383.

Table 1
Volume Flow Rate Correction Calculations
For CR-3 Tube 106-32-2 (1992)

Time	Recorded Pressure	Assumed Flow Rate	Integral Test Volume	Flow Error Model	Corrected Pressure
seconds	psi	in^3/sec	in^3	psi	psi
0.00	0	0.000	0.000	0	0
0.50	1800	0.050	0.013	0	1800
1.50	3700	0.050	0.063	0	3700
2.94	6000	0.050	0.134	0	6000
3.18	6450	0.050	0.146	0	6450
3.88	6600	0.050	0.181	0	6600
5.33	8000	0.340	0.464	6	7994
6.50	9420	0.575	1.002	18	9402
7.03	10000	0.680	1.331	26	9974
7.50	10500	0.775	1.677	35	10465
8.00	10920	0.875	2.089	45	10875
8.50	11100	0.975	2.552	57	11043

Note: 2.552 final integral test volume - 0.146 integral test volume at yield = 2.405 cu.in., in agreement with 2.233 cu.in. of test volume calculated based on sample length and post test diameters.

Table 2
Estimates of Burst Pressure Based on Defect Geometry

Tube	41-44-2	97-91-2	106-32-2
IGA Depth	16.7 mils	20.0 mils	14.8 mils
IGA Axial Length	70 mils	76 mils	63 mils
1994 Baseline Burst Pressure	10,100 psi	10,450 psi	11,250 psi
Burst Pressure Δ, Uniform Thinning[1]	620 psi	965 psi	515 psi
1994 Defect Burst Pressure Δ	300 psi	-	-

Δ: The given pressures are the baseline burst pressure minus the defect burst pressure.

1: Burst pressure calculated assuming the defect to be a region of uniform thinning of length equal to the IGA axial length, and which extends completely around the circumference of the tube. This is conservative modelling. Calculations adapted from Reference 3; nominal dimensions assumed.

Table 3
Summary of Burst Pressure Estimates Using Three Independent Methods

Tube	97-91-2	106-32-2
1994 Baseline Burst Pressure	10,450 psi	11,250 psi
1992 Working Fluid	Hydraulic Oil	DI-water
1992 Burst Pressure, Unadjusted	12,400 psi	11,100 psi
Flow Rate Corrected	N/A	11,040 psi
Predicted by Defect Geometry	9,485 psi	10,735 psi
Estimated by Diametrical Strain	10,300 psi	10,915 psi

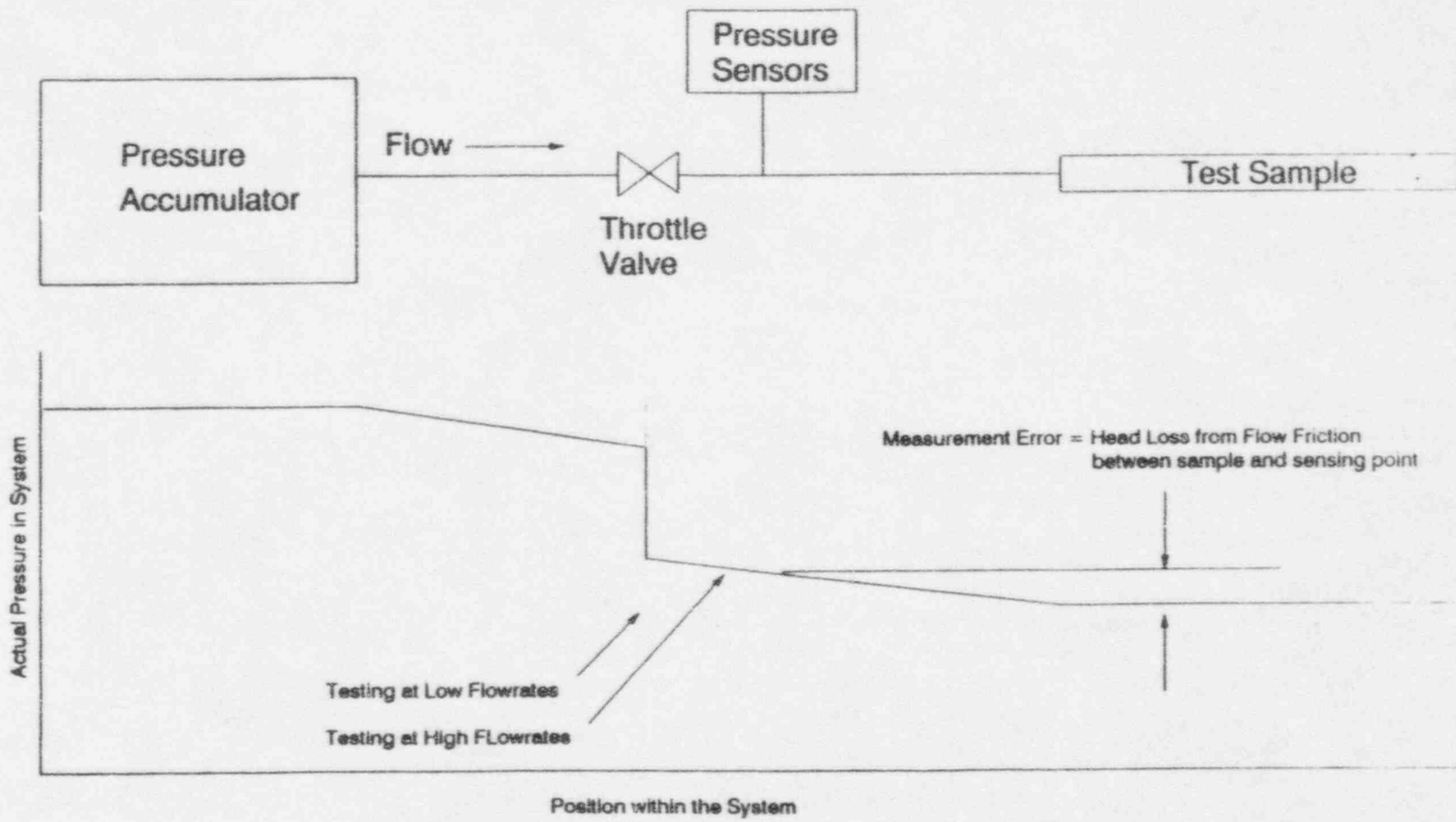

Figure 1: Schematic of the burst test apparatus, below which is a graph of pressure versus position within the system. At high flow rates, flow friction gives rise to a measurable pressure drop (head loss) in the small diameter, high pressure tubing that transfers the hydraulic fluid from the accumulator to the test sample.

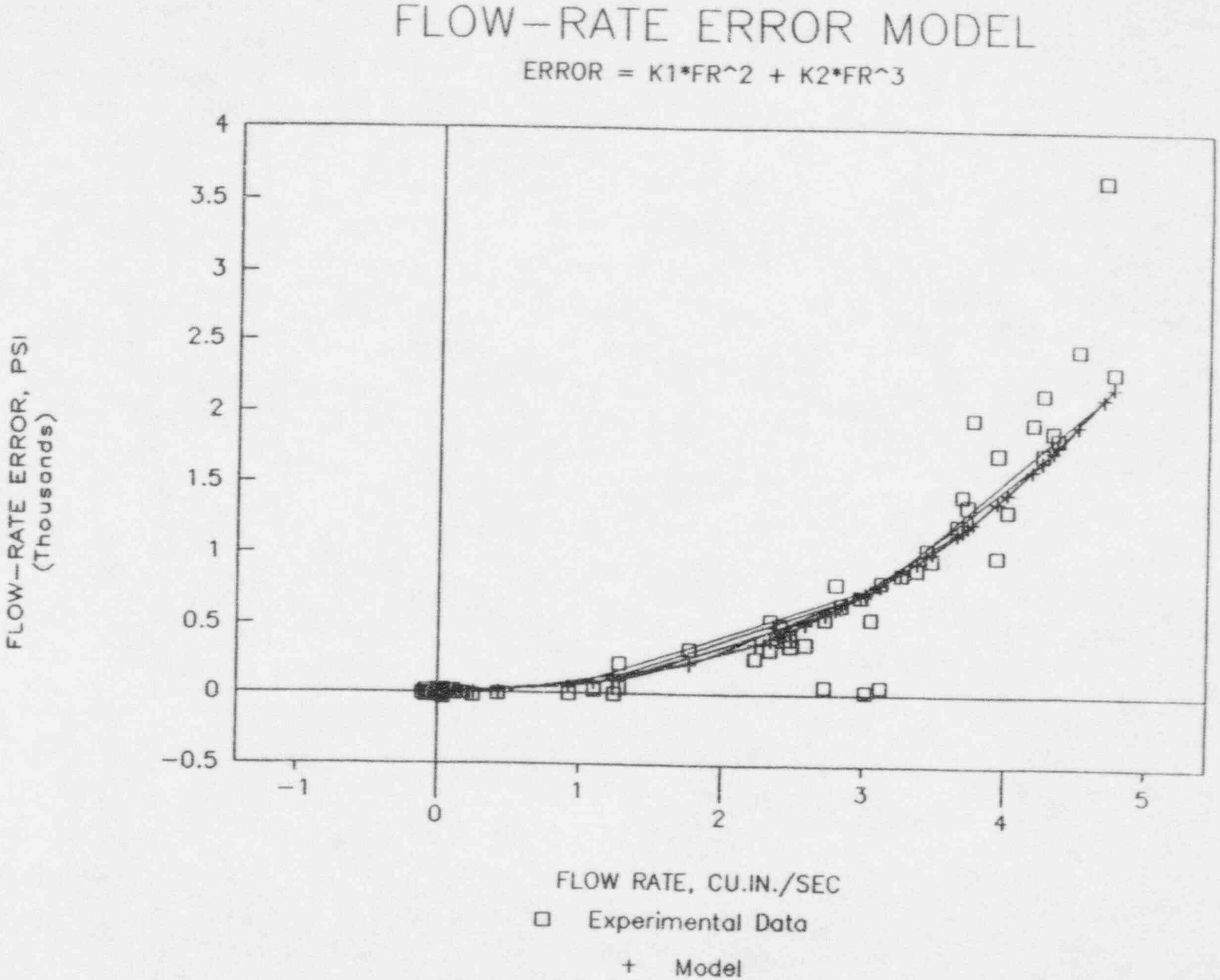

Figure 2: Graph of experimentally determined error in pressure caused by flow friction as a function of flow rate. The equations used to model the behavior is also shown.

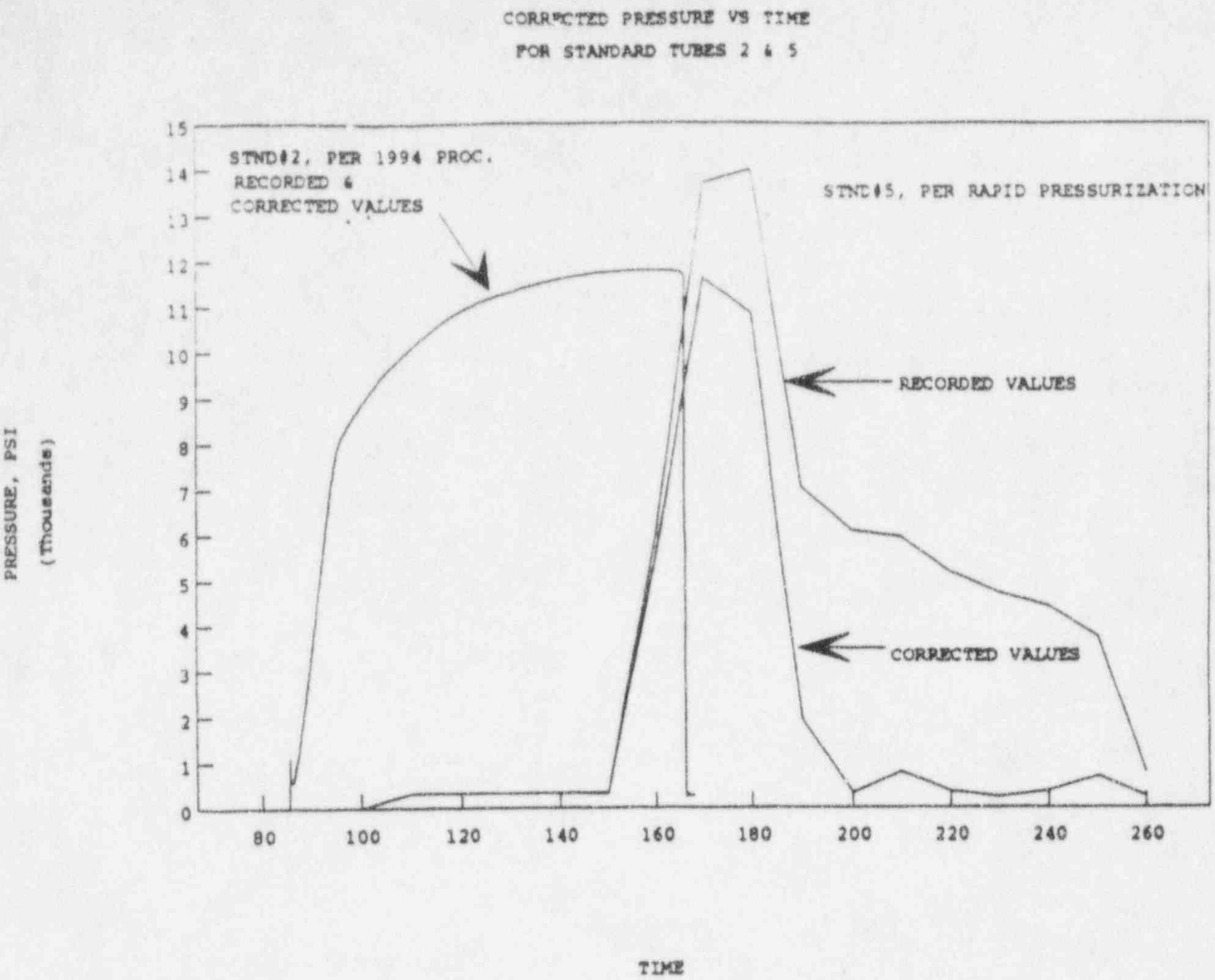

Figure 3: Application of the flow rate error model to pressure versus time data of burst testing of virgin S/G tubing. The curve on the left (time units = seconds) is from testing per 1994 procedures. Because of the low flow rates, no significant flow rate error is predicted, and the curve on the left is actually the overlapping uncorrected and corrected data. The curves on the right (time units = 1/100's of seconds) is from testing at high flow rates. The model predicts several thousand psi of error at the flow rates used, and corrects the pressures downward into agreement with the data from testing per 1994 procedures. Note that the uncorrected data show 3 to 7 thousand psi of flow rate error after sample burst has occurred (from time units 200 to 240), which is corrected to nearly zero by the corrected curve.

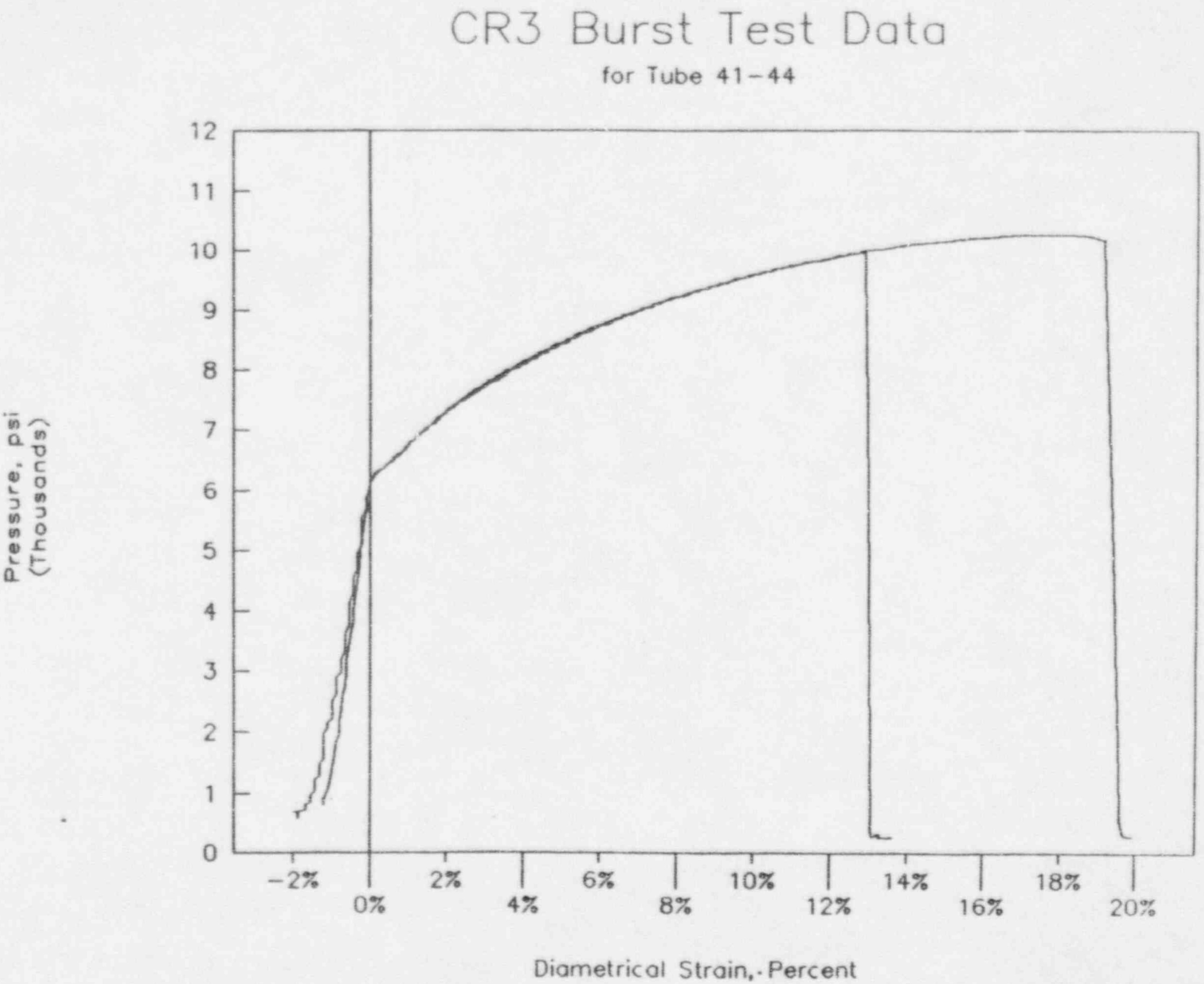

Figure 4: Pressure versus Diametrical Strain graph of burst test data for samples 41-44-2 (small IGA patches) and 41-44-5 (defect free).

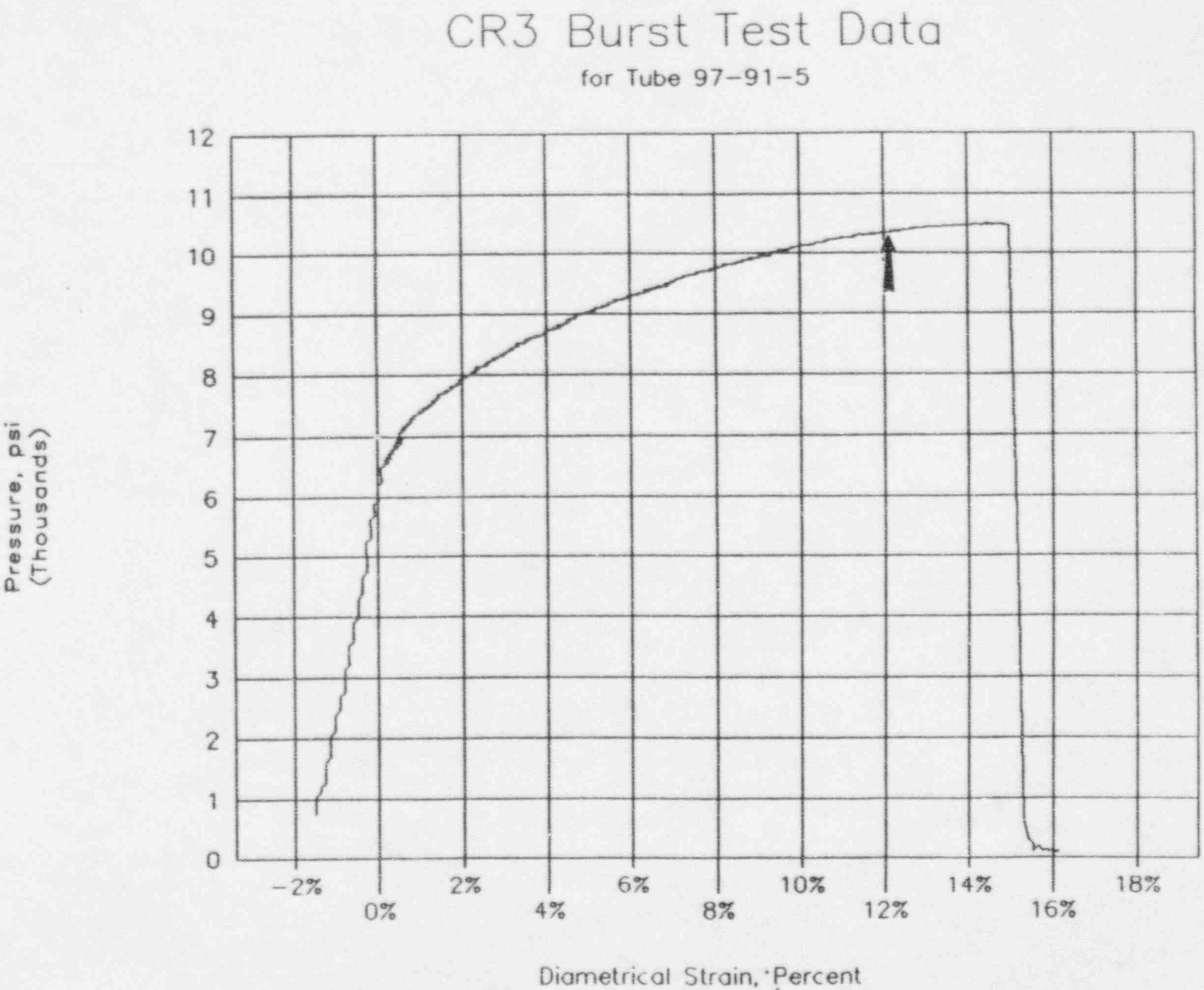

Figure 5: Pressure versus Diametrical Strain graph of burst test data for sample 97-91-5 (defect free). The arrow indicates the 12.1% strain at which sample 97-91-2 burst in 1992 testing. This corresponds to a burst pressure of 10,300 psi.

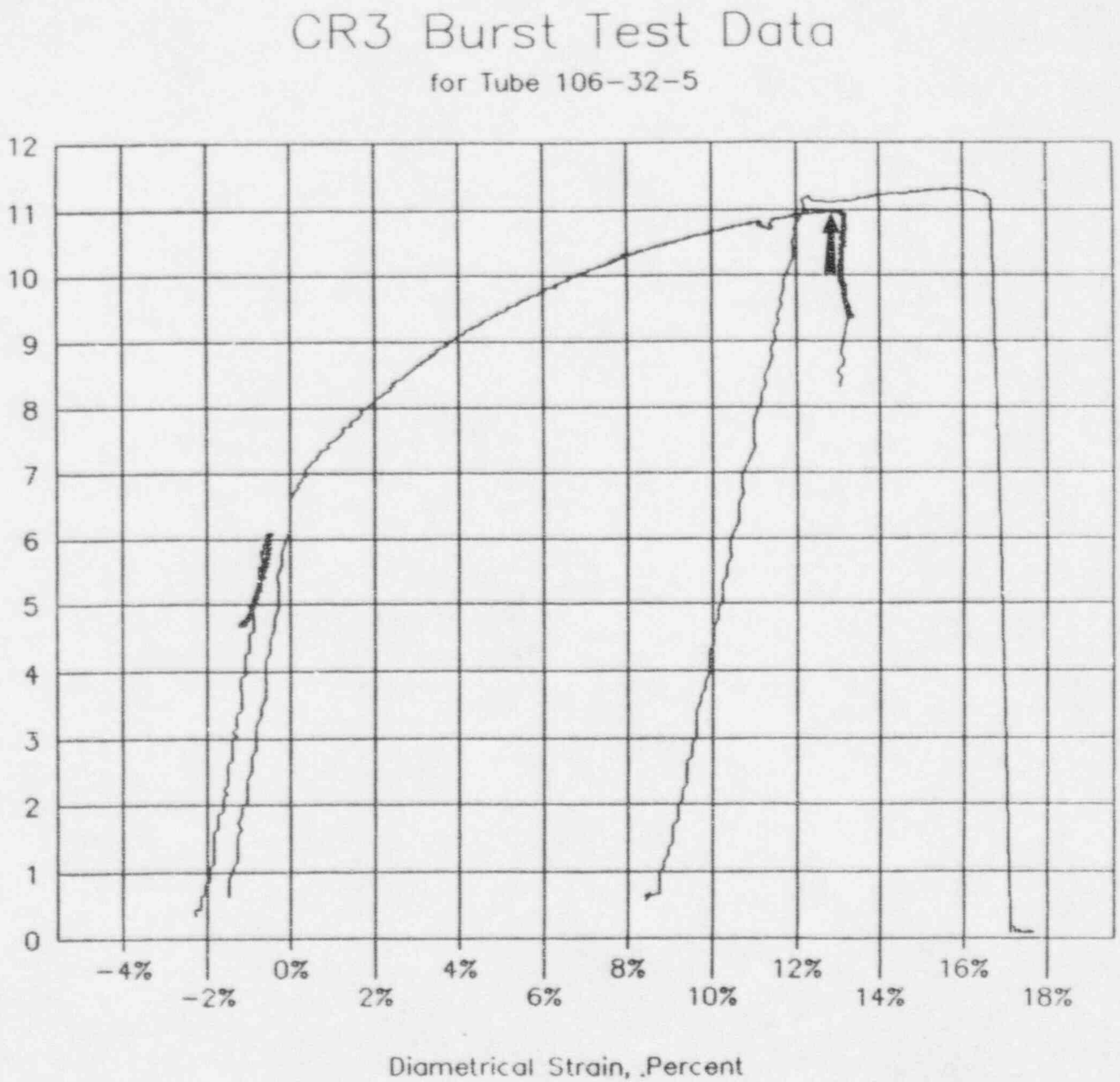

Figure 6: **Pressure versus Diametrical Strain graph of burst test data for sample 106-32-5 (defect free). The arrow indicates the 12.9% strain at which sample 106-32-2 burst in 1992 testing. This corresponds to a burst pressure of 10,915 psi.**

APPENDIX B

INDUSTRY EXPERIENCE WITH TUBE WEAR

APPENDIX B

DESCRIPTION OF AND INDUSTRY EXPERIENCE WITH STEAM GENERATOR TUBE WEAR

Description

Wear is defined as the volumetric removal of material caused by the mechanical action of one material in contact with another. Wear cuts across grains nondiscriminantly leaving a surface similar in appearance to one formed by general corrosion (Reference 1). Tube wear geometry is generally controlled by the shape, orientation, and inclination of the secondary-side structural object adjacent to the tube. In Westinghouse units, wear was first confirmed at AVB's on tubes removed from San Onofre-1 during 1974 (Reference 2) and at outer periphery tube support plates in the preheater section on tubes removed from Ringhals 3 in 1981 (Reference 3). Wear in Combustion Engineering units was first confirmed at support straps on tubes removed from Calvert Cliffs in 1983 (Reference 4). Wear was first observed in Babcock & Wilcox once-through units at upper span broached tube support plates on a lane region tube removed from Oconee-2 in 1977 (Reference 5).

Morphologies Observed

Examples of variations in wear scar geometry as observed on pulled tubes are shown in Figures 1 through 3. Wear scar shape is strongly controlled by the inclination of the tube relative to the adjacent support structure; for inclination angles near zero degrees, the wear shape is rectangular while for non-zero inclination angles, the shape becomes triangular. Figure 1 shows examples of a rectangular shaped morphology for tubes removed from recirculating and once-through steam generators. Figure 1(a) shows an example of an AVB wear scar on a tube removed from Zion-2 (Reference 6). The rectangular AVB bar used in Westinghouse units tends to create rectangular, non-tapered wear scar flats. AVB wear scars may be oriented perpendicular to the tube longitudinal axis or may be slightly oblique as shown in the figure depending on the alignment of the AVB bar relative to the tube. An example of a rectangular shaped wear scar geometry for tube wear at baffle plates in Westinghouse preheater steam generators for tubes removed from Almaraz-1 (Reference 7) is shown in Figure 1(b). Rectangular wear scar morphology for tube wear at a broached tube support plate land contact area (LCA) in Babcock & Wilcox OTSG's is shown in Figure 1(c). For this example, the scar assumes the shape of the land contact area; it is relatively flat because of a near-zero inclination angle. Figure 2 shows examples of triangular shaped wear scars as observed on tubes removed from recirculating steam generators. In addition to being triangular in shape, the wear scar is generally tapered due to non-zero inclination angles. Figure 2(a) shows wear that occurred at a 4-inch support strap on a tube removed from Calvert Cliffs-1 (Reference 4). In this case, the triangular shape is determined by edge oscillation of the thick support strap. An example of a

triangular-shaped wear scar geometry for tube wear at baffle plates in Westinghouse preheater steam generators for a tube removed from Almaraz-1 (Reference 7) is shown in Figure 2(b). The imprint of the baffle plate hole drill marks transferred to the tube outer surface can be seen in the figure.

An example of an oval or pit-like wear morphology as observed on tube R49C48 removed from Almaraz-1 (Reference 8) is shown in Figure 3. An oval shaped wear cavity was observed at the lower edge of the fourth cold-leg baffle plate intersection. The cavity is described as mechanically induced, possibly due to wear with an object wedged into the tube baffle annulus. The dimensions of this type of wear will be determined by the size of the particulate matter distributed on the steam generator secondary side. For the example shown in the figure, the oval shaped cavity was 0.015-inch deep; again, the cavity is mechanically induced and not due to corrosion.The occurrence of this morphology is relatively rare; it has been observed in both active and inactive forms distinguished by the presence or absence of deposits or scale within the pit.

Extent of Occurrence

Tube wear generally continues to occur as an active damage mechanism in steam generators of all NSSS designs. However, it is viewed as nuisance degradation rather than a threat to steam generator lifetime or tube integrity. In Westinghouse preheater steam generators, significant tube wear at baffle plates within the preheater section has essentially been abated with the implementation of plant corrective actions. Tube wear at AVB's continues in a large fraction of Westinghouse type units with some units having had their original AVB's replaced with an improved design intended to retard tube wear. Tube wear at support straps and batwings, and at baffle plates within the economizer section of System 80 steam generators, represent the largest percentage of repaired tubes in Combustion Engineering units. However, most of these tubes have been plugged preventatively. In Babcock & Wilcox units, broached support plate tube wear has been diagnosed in the majority of units; however, growth rates are generally small accounting for only a very small fraction of the total plugged tube population.

Outages Caused by Wear

Tube wear has caused relatively few forced outages. Of the several hundred forced outages that have occurred due to tube degradation, only four can be attributed to wear. This small number is attributed to slow growth rates and ready detection of wear by conventional NDE techniques. Where forced outages have occurred, the cause has been attributed to steam generator sample plan inadequacies. In recirculating units, the first occurrence of a forced outage attributable to wear was at Ringhals-3 in 1981 with the most recent occurrence at Palo Verde-1 in 1987. No forced outages have occurred in once-through steam generators because of tube wear.

Industry NDE Experience

Eddy current is by far the most common tube examination method with the bobbin and rotating probe being the two most common techniques. Regular-shaped mechanical degradation such as wear is usually detected and sized using a bobbin coil *absolute mode* analysis technique. Wear is sometimes tapered, and the absolute mode is more sensitive to this condition. Depth sizing is accomplished using wear scar standards that replicate the geometry of the tube wear. Irregular-shaped mechanical degradation when detected with the bobbin probe is sized using conventional phase angle analysis procedures.

No significant issues exist with regards to the NDE of wear. Existing bobbin probe eddy current techniques adequately detect and size wear with detection at 20% through-wall and a sizing error of approximately 10% through-wall. Tube wear is a relatively large volume defect readily detectable using standard bobbin coil technology. Eddy current signal amplitude sizing techniques *using wear scar standards that replicate wear morphology* are typically used to size regular wear geometries while conventional phase angle analysis is used for irregular or pit-like geometries.

Bobbin probe detection and depth sizing experience for recirculating steam generator wear scars is shown in Figure 4. For detection (see Figure 4(a)), the transition between detection and non-detection is rather narrow occurring at a depth approximately 20% through-wall. Eddy current bobbin probe depth sizing accuracy is shown in Figure 4(b). The data set (61 data points) are described by the regression equation $Y = 0.94 * X + 3.1$ with a correlation coefficient of $R = 0.97$ and a standard error is 3.9%.

Detection and sizing experience for wear in once-through steam generators is comparable to recirculating steam generator experience. Wear at broached support plates occurs at the land contact areas as illustrated with the rotating probe eddy current graphic shown in Figure 5(a) which shows a wear scar indication located at one of the lands. Eddy current pancake coil data acquisition and analysis techniques are used to selectively isolate individual wear scars at each of the lands for improved depth sizing thus avoiding bobbin probe averaging effects (References 8-9). This is illustrated with the sizing data shown in Figure 5(b) generated using laboratory data. The data set (18 data points) is described by the regression equation $Y = 0.97 * X - 0.14$ with a correlation coefficient $R = 0.97$. The standard error is 2.6%.

References

1. Steam Generator Reference Book. Electric Power Research Institute, Palo Alto, CA., May 1985.

2. Pement F.W., et. al., "Examination of San Onofre Steam Generator C Tube (46-61) and Anti-Vibration Bar," Westinghouse R&D Report 77-7D2-SGEXM-R8, August, 1977.

3. Rosborg, B., "Ringhals 3; Fretting Defects on Steam Generator Tubes," Studsvik Energiteknik AB Report ET-81-141, 1981.

4. Rudell, B.C., and D.J. Van Petten, Destructive Examination of Steam Generator 11 Tubing at Calvert Cliffs Power Plant Unit 1, EPRI Report NP-7136-SD, April 1991.

5. "Tube Damage - Once-Through Steam Generators," Corrosion Advisory Committee Meeting, EPRI, Feb. 1978.

6. Aspden, R.G., and F.W. Pement, Destructive Examination of Zion Unit 1 Tube and Antivibration Bar Samples, EPRI NP-4375-LD, December, 1985.

7. Pement, F.W., et. al., "Almaraz Unit 1 Examination of Tubes R49C42 and R49C74 From Steam Generator No. 1," Westinghouse Report WCAP 10038, January 1982.

8. J. M. Gilkison "Preliminary Report of the Non-Destructive Examination of Tubes R49C48 and R49C53 From Steam Generator No. 3 - Almaraz Unit 1." April 1982.

9. Workshop Proceedings: Fretting and Wear Susceptibility in Nuclear Steam Generators, March, 1986, Washington, D.C.

10. Pendergrass, S.C., and J.B. Watkins, "Multi-Element Eddy Current Technique For the Evaluation of Wear Fretting at Broached Support Plates in Nuclear Steam Generator Tubing," 8th International Conference on NDE in the Nuclear Industry, Kissimmee, Florida, November 1986.